AD NUMBER
AD378636
CLASSIFICATION CHANGES
TO: unclassified
FROM: confidential
LIMITATION CHANGES
TO: Approved for public release, distribution unlimited
FROM: Distribution: Further dissemination only as directed by Director of Supersonic Transport Development, Federal Aviation Agency, Washington, DC 20553, 15 NOV 1965, or higher DoD authority.
AUTHORITY
FAA ltr, 23 Feb 1972; FAA ltr, 23 Feb 1972

NOTICES

When Government drawings, specifications, or other data are used for any purpose other than in connection with a definitely related Government procurement operation, the United States Government thereby incurs no responsibility nor any obligation whatsoever; and the fact that the Government may have formulated, furnished, or in any way supplied the said drawings, specifications, or other data, is not to be regarded by implication or otherwise as in any manner licensing the holder or any other person or corporation, or conveying any rights or permission to manufacture, use, or sell any patented invention that may in any way be related thereto.

All distribution of this document is controlled. In addition to security requirements which apply to this document and must be met, it may be further distributed by the holder only with specific prior approval of:

Director of Supersonic Transport Development
Federal Aviation Agency
Washington, D. C. 20553

The distribution of this report is limited because it contains technology identifiable with items excluded from export by the Department of State (U. S. Export Control Act of 1949, as amended).

UNCLASSIFIED

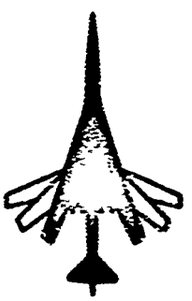

AIRCRAFT PROPULSION SYSTEM

COMMERCIAL SUPERSONIC TRANSPORT PROGRAM

PHASE II-C

INTERIM AIRCRAFT PERFORMANCE ASSESSMENT REPORT

NOVEMBER 15, 1965
CONTRACT FA-SS-66-5

THE BOEING COMPANY
RENTON, WASHINGTON, U.S.A.

D6-19903

ISSUE No. 8

UNCLASSIFIED

CONTENTS

CONTENTS (Cont.)

ILLUSTRATIONS

ILLUSTRATIONS (Cont.)

TABLES

1.0 SUMMARY

This document describes the propulsion system for the Model 733-390 airplane using the 475-pounds-per-second General Electric GE4/J5G afterburning turbojet as the primary engine selection. This selection is retained from Phase II-A because of the GE engine superiority in economics, performance, and growth potential. Since Phase II-A, no changes in the performance, costs, or growth of the General Electric or Pratt & Whitney engines have occurred which would alter relative evaluation.

Supplement I of this document describes installation, performance, and noise data for the P&WA JTF17A-20B engine. The Pratt & Whitney engine can be installed in the airplane with a minimum of change. Installation studies, performance analyses, and coordination with both engine contractors are being pursued during Phase II-C.

This document deals with the changes and improvements made during Phase II-B and II-C to the propulsion system of the Model 733-290. All parts of the propulsion system not specifically mentioned remain unchanged and are as described in D6-8880-8, (Phase II-A Aircraft Propulsion System).

1.1 ENGINE INSTALLATION

- The engine afterburner is straight rather than bent 8 degrees. This change directs the exhaust gas above the horizontal tail.
- The engine fuel accessories are located on the top centerline of the engine in the wing cavity, with the lubrication and hydraulic components in a small capsule on the engine bottom. This arrangement ensures the minimum nacelle frontal area, minimizes pod drag, and improves the safety aspects of a wheels-up landing.
- The engine front frame has been extended to provide space for the secondary air valving and control and the forward front mount system.
- A pressurized pod carries the nozzle secondary air from the inlet to the nozzle. This design reduces the nacelle frontal area and requires a redesign of the fire protection system. (Fig.) shows the pod general arrangement.)

1.2 INLET SYSTEM

- The subsonic diffuser lines have been modified slightly to improve the efficiency of the bypass system.
- Vortex generators have been added to the cowl to further reduce inlet distortion.
- The normal shock position indicator system has been redesigned to be directly controlled by the inlet aerodynamics rather than by servovalve position.

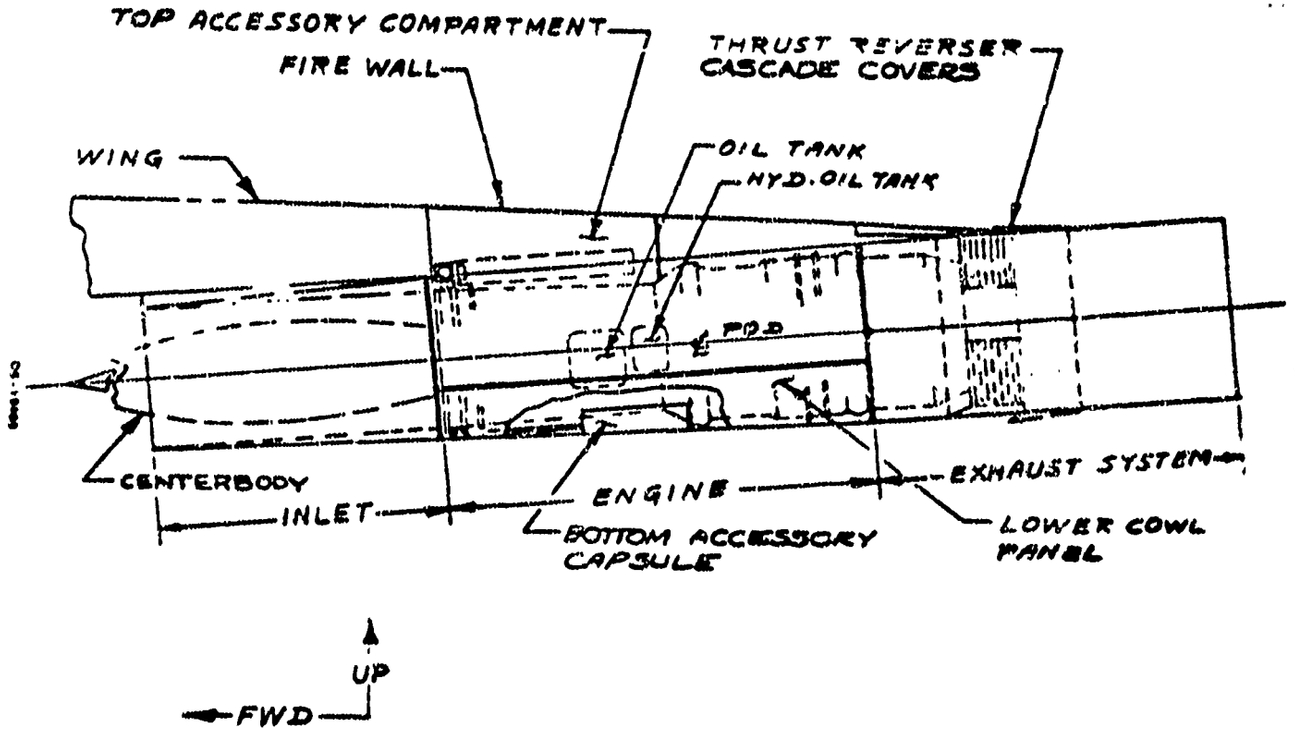

Fig. 1 Pod General Arrangement

- The pressure taps for the restart sensor have been relocated to ensure a better signal.
- A buzz warning light has been installed on the flight engineer's panel.
- Substantiating test data have been obtained on the suitability of the control sensor locations.
- The relative location of the inlet and landing gear has been improved. The gear is longer and is centered between the inlets when extended.

1.3 PROPULSION CONTROLS

- The thrust reverser control has been simplified by the tentative elimination of the null thrust position.
- The open-nozzle concept for noise reduction is used during power cutback after takeoff. This reduces engine noise by 3 PNdb.
- Engine airflow trim during nonstandard days has been revised so that the engine can be trimmed to match the inlet for hot days as well as cold days. Modulation of the nozzle secondary air control valve is used on hot days to bypass more air. This improves the hot-day range of the airplane and increases trimming flexibility for engine and inlet tolerances.

1.4 EXHAUST SYSTEM

Considerable wind-tunnel test data have been obtained on the jet wake characteristics at Mach 2.7; these data have resulted in the relocation of the horizontal tail on the 733-390 configuration. Model tests for thrust reverser reingestion have also been conducted.

1.5 FUEL SYSTEM

- A rearrangement of the tanks reduces body structural weight, fuel system weight, and center-of-gravity travel.
- More efficient use of insulation in Main Tank No. 1 and auxiliary tanks reduces weight and cost and furnishes additional fuel volume.
- Flight cycle environment tests show no fuel tank coke formation. Tanks will remain deposit-free even when minimum quality ASTM D-1655-63T Jet A or A-1 commercial kerosene are used.

2.0 GENERAL DESCRIPTION AND INSTALLATION

The propulsion pods for the 733-390 are designed to fit the General Electric GE4/J5G afterburning turbojet engine. The propulsion pod is similar to the configuration shown on the 733-290 (Phase II-A). Design refinements have been made as the result of many studies, investigations, and tests to improve the propulsion pod.

2.1 POD SHAPE

The location of the propulsion pods on the airplane has not significantly changed, but the overall pod shape has changed from the cambered pod on the 733-290 to a slim, straight pod as shown in Fig. 2. The removal of the 8-degree bend from the afterburner simplifies the engine. The straight pod, mounted tightly to the wing lower surface, directs the exhaust gas above the horizontal tail along the direction of flight. A reduction of 6.6 percent in pod volume has been achieved by relocating the major engine accessories to an area on the engine top centerline and by changing the design of the secondary air system.

2.2 ENGINE ACCESSORIES

All of the engine accessories associated with the fuel system are mounted on a platform on the top of the engine in an unpressurized cavity in the wing as shown in Fig. 2. The engine lubrication oil tank and nozzle hydraulic oil tank are both located on the side of the engine compressor case. All other engine accessories, such as the engine lubrication oil pumps and the nozzle hydraulic pumps and controls, are located on the engine bottom in an unpressurized capsule. A small local bump in the basic pod contour is required to enclose the capsule. The inlet hydraulic pumps are mounted on top of the inlet and driven by a gearbox and shaft located forward of the engine mount.

2.3 SECONDARY AIR SYSTEM

A schematic diagram of the secondary air system is shown in Fig. 3. The secondary air enters the cowl cavity through a number of flow control valves located in the engine front frame. These valves, and their control system, are provided as an integral part of the engine. At static and low flight speed conditions, the secondary air is taken in through a number of air supply doors located in the aft cowling.

This change effectively pressurizes the cowl cavity in flight to a maximum of 10 psi above ambient. The cowl panels have been redesigned to be tightly sealed and withstand the pressure loads (Fig. 4 is a schematic of the cowl design).

2.4 FIRE PROTECTION

The Phase I proposal (Par. 2.10, Document D6-2400-12, Volume A-VI, Propulsion) described the proposed engine compartment fire protection system. The basic concept of engine compartment fire protection described in that section remains unchanged. Passing the secondary air for the engine nozzle through the cowl cavity and the

resulting pressurization of that cavity have necessitated redesign of the fire detection and fire extinguishing systems operation.

The propulsion pod is now divided into three areas by sealed firewalls as shown in Fig. 5. These areas are the cowl cavity, which is pressurized by the secondary air, and the top and bottom accessory capsules, which are not pressurized.

For fire control purposes, the accessory capsules at the top and bottom as well as the cowl cavity are considered as one fire zone. The fire extinguishing agent will be discharged simultaneously into the accessory capsules at top and bottom as well as into the cowl cavity. The amount distributed to each area will be controlled by the line and nozzle sizes. An approved, quick-acting fire-detector system will be installed on the engine. A fire or overheat condition will activate the system.

To provide a nonpressurized cowl cavity for efficient fire extinguishing, actuation of the fire switch will close the secondary air control valves located on the engine inlet. This will reduce the cowl cavity pressure to ambient and reduce the air flow through the cavity to a minimum.

Fire pressure relief in a controlled path will be provided by burn-through panels in the secondary air supply doors located in the aft cowling. These panels are designed to also provide pressure relief in the event of secondary air system control malfunction.

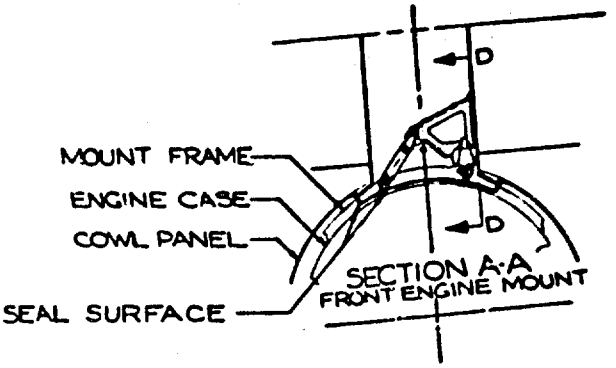

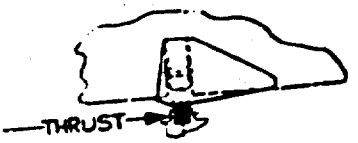

SECTION D-D

ACCESS

SECONC
CONTR

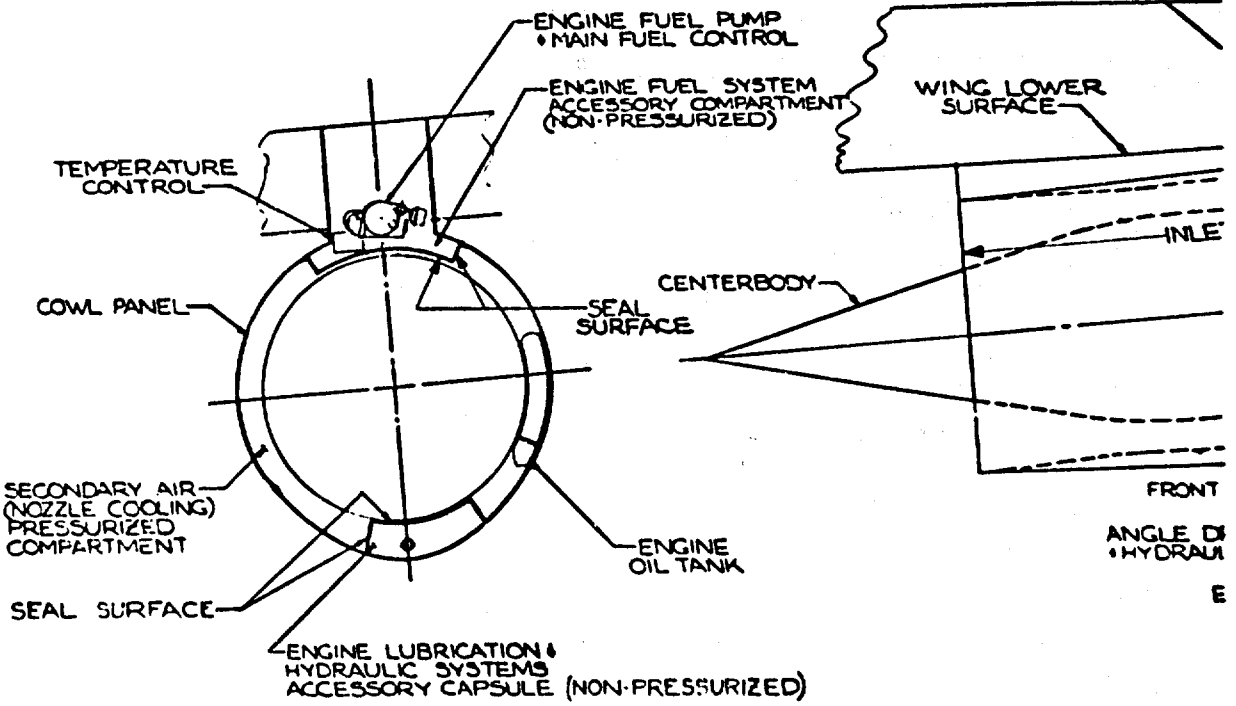

SECTION B-B

ANGLE DI
& HYDRAU

E

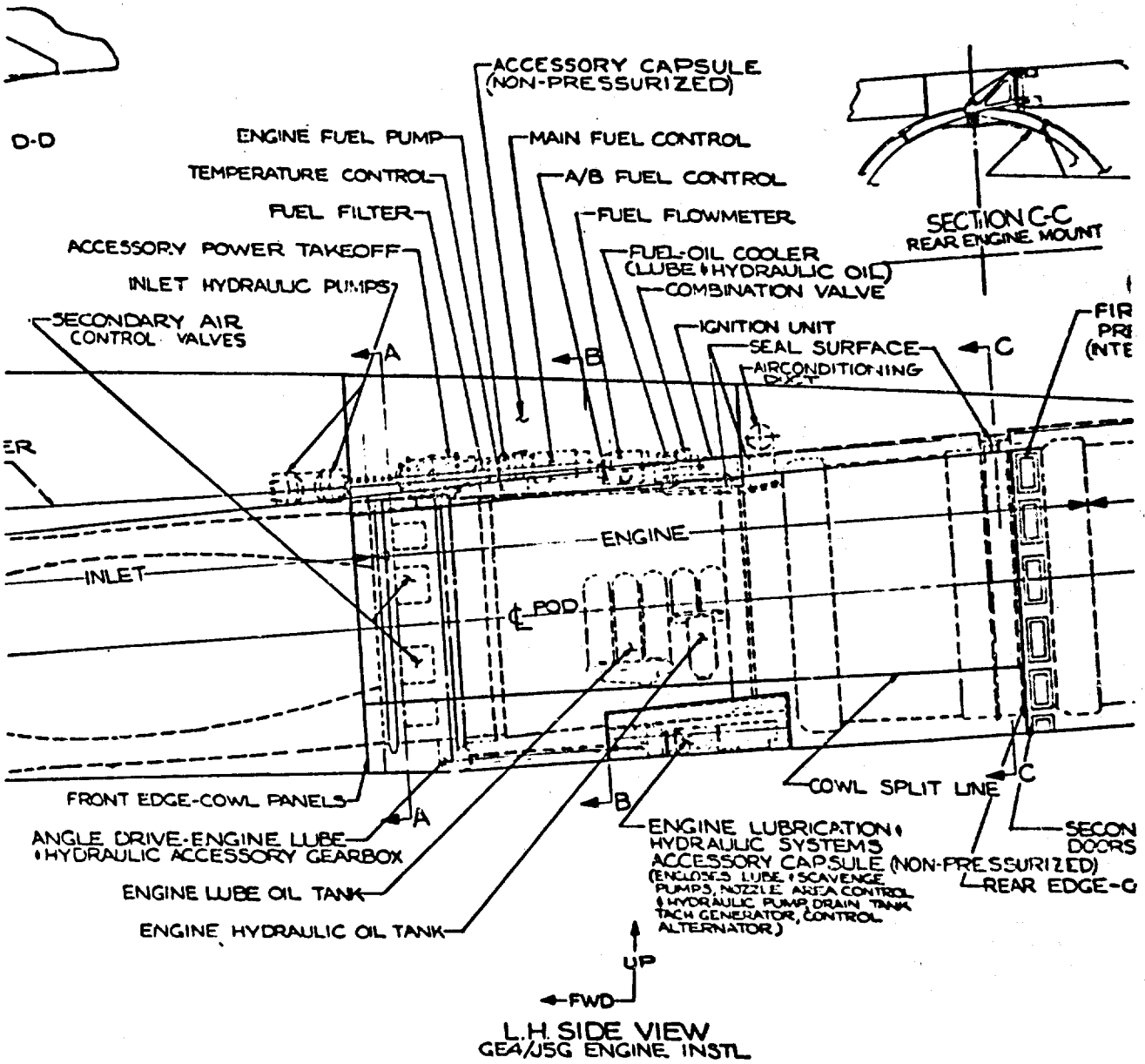

Fig. 2 Propulsion Pod

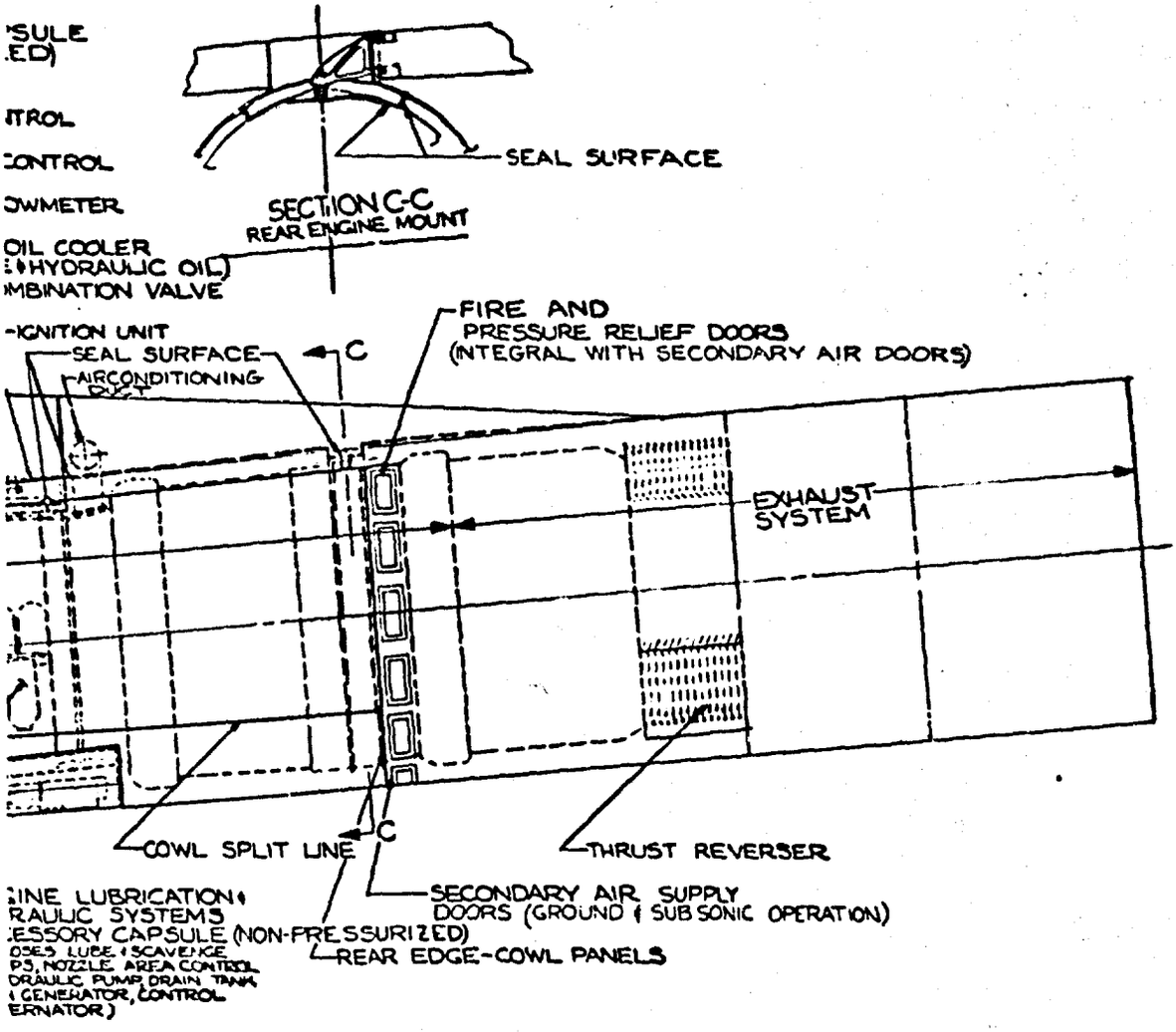

Fig. 2 Propulsion Pod

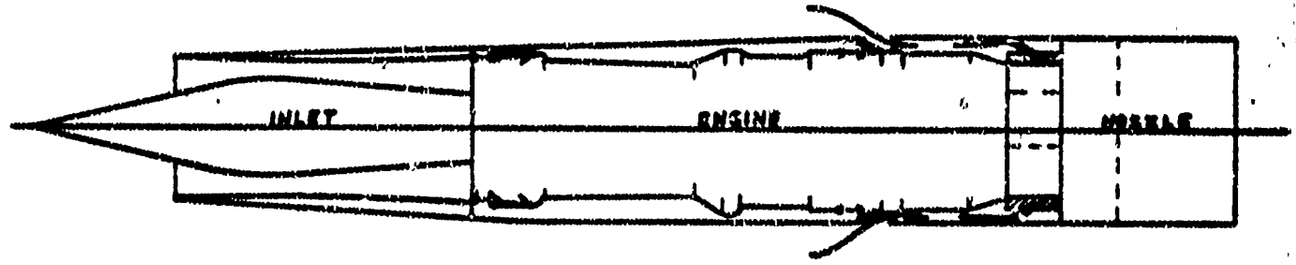

STATIC AND LOW SPEED OPERATION

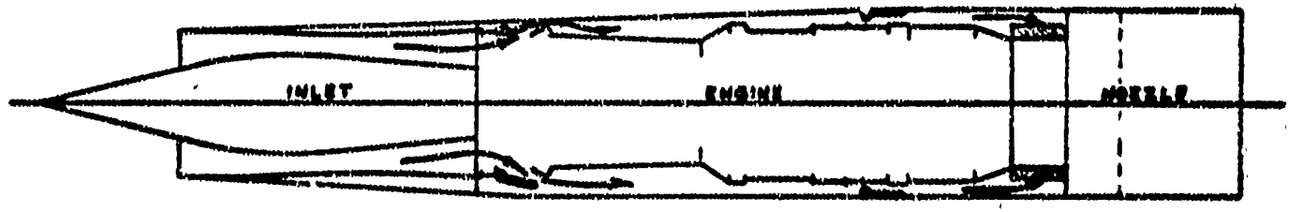

OPERATION ABOVE 0.4 MACH

Fig. 3 Secondary Air System Operation

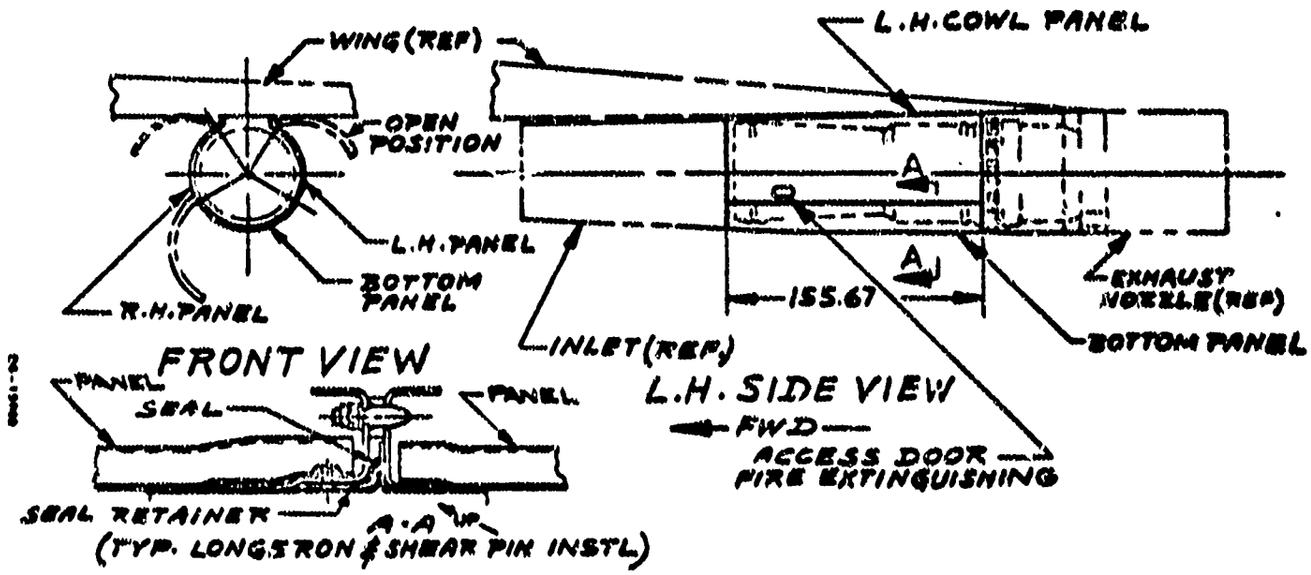

COWLING DATA:

NUMBER OF PANELS:	3		
AREA OF PANELS:	186	SQ.FT. - 62	SQ.FT./PANEL
WEIGHT OF PANELS:	420	LB. - 140	LB / PANEL

Fig. 4 Engine Cowling Schematic

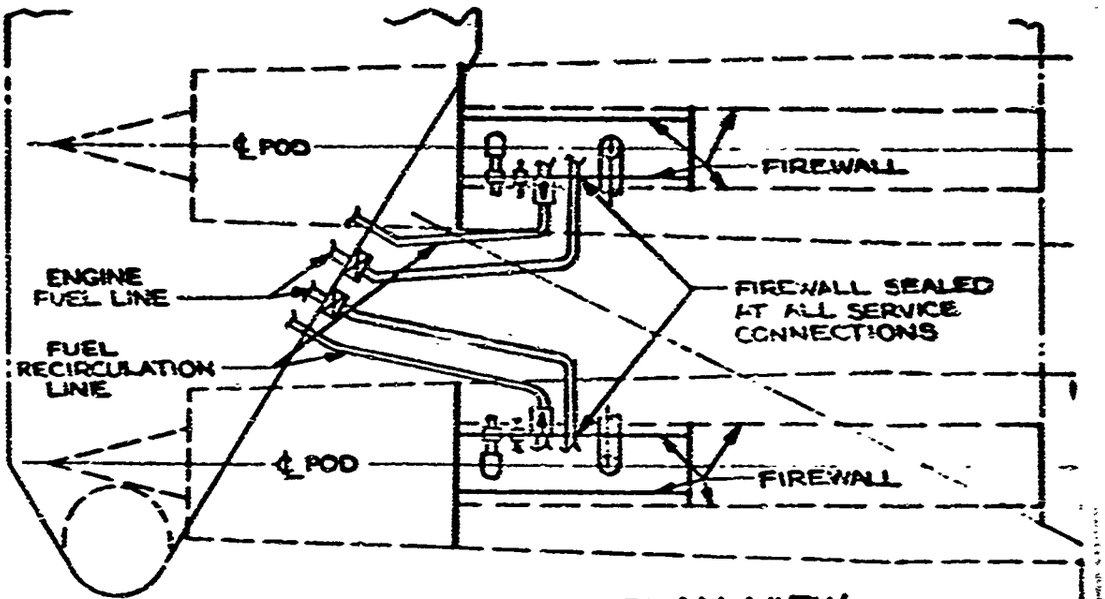

PLAN VIEW

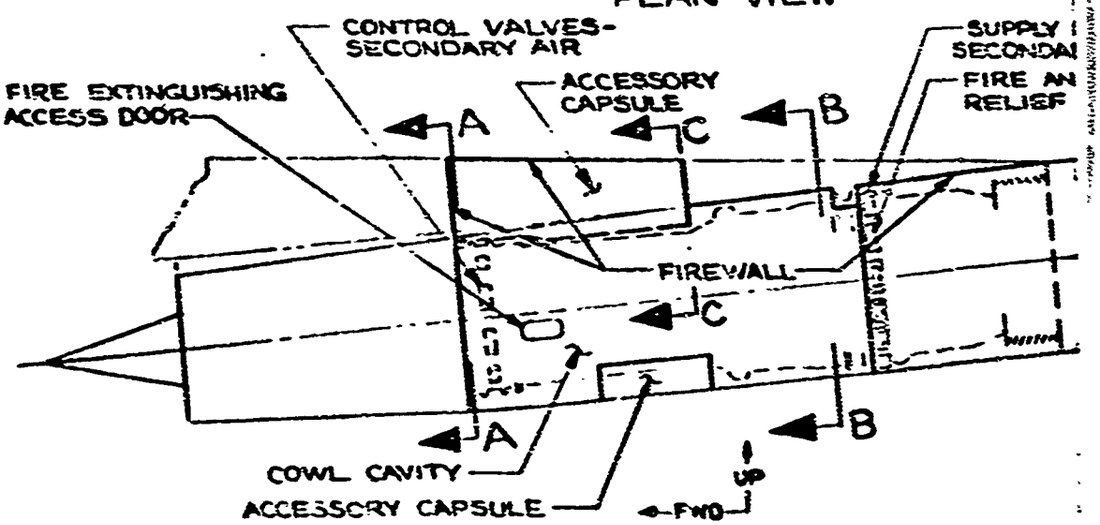

L.H SIDE VIEW
PROPULSION POD

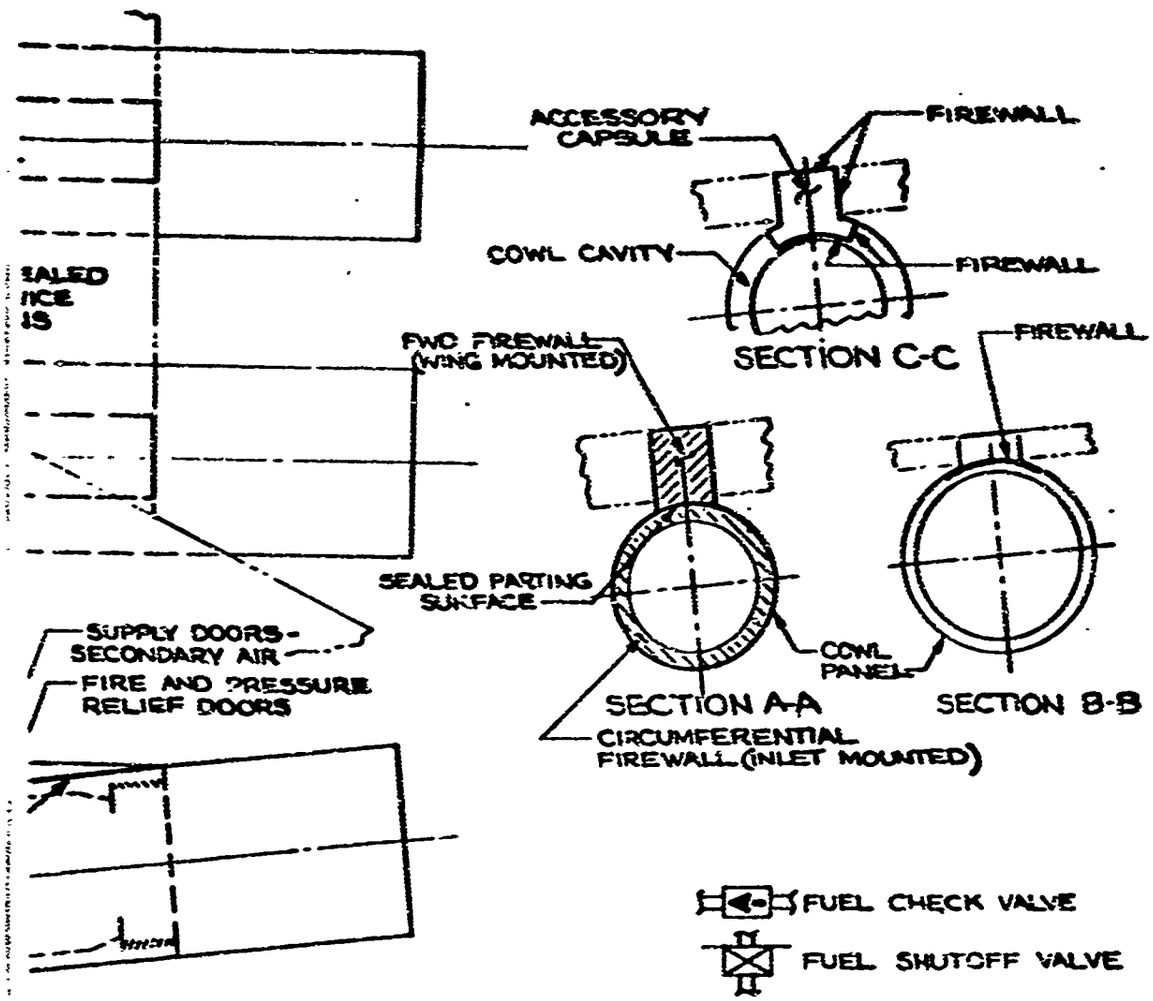

Fig. 5 Fire Protection Schematic

3.0 INSTALLED PERFORMANCE AND WEIGHT

The installed performance of the GE4/J5G engine installation is presented in Document D6-19906-1, Propulsion System Performance Specification dated November 1, 1965. The engine performance data and installed inlet and nozzle drags are essentially the same as those described in Section 9.0 of D6-8680-8, Volume VIII-A, Aircraft Propulsion Systems (Phase II-A Report).

3.1 AIR INDUCTION SYSTEM EFFECT

Refined analysis of the inlet starting operation has resulted in minor off-design performance changes. The reduced pressure recovery during inlet starting operation (Mach 1.7 to 1.9) results in small net thrust, specific fuel consumption, and inlet drag changes. The inlet recovery and drags are discussed in Section 4.0.

3.2 HOT-DAY CRUISE PERFORMANCE

The hot-day nozzle internal performance at Mach 2.63 cruise is changed slightly to account for the increase in secondary air to the nozzle due to the use of the secondary air system to bypass excess inlet air. Fig. 6 shows the calculated thrust coefficient loss versus amount of secondary air at cruise. Because of the excess secondary air on a hot day, the nozzle thrust coefficient is reduced 0.09 percent, but the overall effect is a range improvement because the inlet bypass drag is eliminated.

3.3 ENGINE INSTALLED WEIGHT

The weight of the GE4/J5G engine at 475 pounds-per-second airflow as designed for the Boeing airplane is 8800 pounds as specified in Ref. 1. This weight includes special features required for installation of the engine in the Model 733-390 airplane. Since the Phase II-A submittal, the changes to the engine which have affected weight are:

- Relocated fuel and hydraulic accessories (top and bottom)
- Front frame extension and modification of the secondary air system and front mount design
- Redesign of secondary air system, including valves and controls

The following Boeing installation features are included in the installed engine weight:

	Pounds
Mounting Strut	129
Engine Mounts	95
Wing Attachment Fittings	180
Firewall and Seals	30
Brackets and Supports	15
Miscellaneous	43
Engine Weight	8800
TOTAL INSTALLED ENGINE WEIGHT	9295 pounds

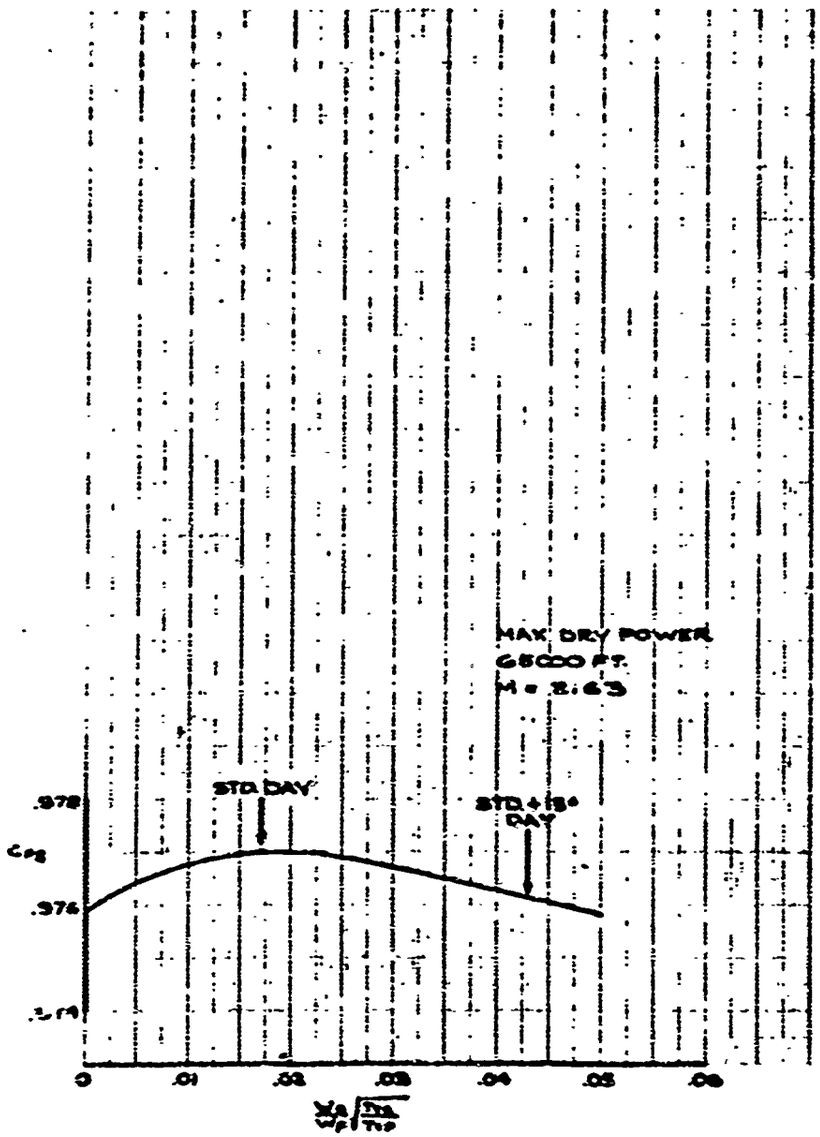

Fig. 6 Nozzle Thrust Coefficient

Total installed propulsion pod weight is:

	Pounds
Inlet	1,755
Cowling	420
Installed Engine	9,295
TOTAL PROPULSION POD WEIGHT	11,470 pounds

3.4 ENGINE CHARACTERISTICS

Table A shows the design characteristics of the engine.

3.5 ENGINE PERFORMANCE

The guaranteed performance for selected flight conditions is contained in Ref. 1. For all other operating conditions the computer deck (Ref. 2) provides the estimated performance with installation corrections. Performance data are based on the 1962 U.S. Standard Atmosphere and geometric altitude.

Table 4 Engine Characteristics

Sea-Level Static Standard Day Thrust (No Losses) (pounds)	
Maximum Augmented	41,800
Maximum Dry	30,700
Engine Dry Weight, Including Exhaust Nozzle and Thrust Reverser (pounds)	8,800
Thrust-to-Weight Ratio (Sea Level Static)	
Maximum Augmented	4.8
Maximum Dry	4.4
Net Thrust-to-weight Ratio (Transonic Mach = 1.2, 45,000 feet)	
Maximum Augmented	2.0
Design Mach Number	2.7
Supersonic Cruise SFC	
Mach 2.7, 65,000 feet	
Ram Recovery = 0.90	1.43
Subsonic Cruise SFC	
Mach 0.8, 40,000 feet	
Ram Recovery = 0.985	1.08
Loiter SFC, Mach 0.43, 15,000 feet	
Ram Recovery = 0.986	1.3[illegible]
Acceleration Net Thrust (pounds)	
Mach 1.2, 36,150 feet	27,200
45,000 feet	17,700
55,000 feet	10,900
Reverse Thrust (Percent Maximum Dry Power)	50
Turbine Inlet Temperature (Nominal) (°F)	
Takeoff	2,200
Supersonic Cruise	2,200
Transonic Acceleration	2,200
Augmentation Temperature (Nominal) (°F)	
Takeoff	1,980
Supersonic Cruise	2,500
Transonic Acceleration	3,000
Compressor Pressure Ratio	9.5:1
Initial Time Between Overhaul (hours)	600 to 1000

4.0 AIR-INDUCTION SYSTEM

4.1 INLET DESIGN

The inlet is basically the same as that proposed in the Phase II-A submittal. Minor changes have been incorporated to improve the design in various areas.

Vortex generators are now used on the cowl wall of the subsonic diffuser in addition to those on the centerbody to reduce further the distortion level of the inlet and to achieve better off-design operation.

The subsonic diffuser is changed in two areas: (1) the contours are modified to account for changes in strut shape and thickness at the diffuser exit, where the inlet struts mate with the engine front frame struts; and (2) the hinge points of the centerbody are relocated to improve the diffusion with the centerbody fully contracted. This results in better diffusion and lower Mach numbers ahead of the bypass doors when the centerbody is contracted.

To improve the entry of takeoff air, the rear lip of the bypass section has been redesigned, and the bypass door actuators are relocated forward of the opening. The engine front frame has been extended forward. This increases the distance between the bypass (takeoff) door opening and the compressor face by about 6 inches. Low-speed testing has shown that this improved shape of the lip and the added length to the compressor face are beneficial in reducing distortion.

A schematic drawing of the inlet is shown in Fig. 7. Flow areas and Mach numbers in the diffuser for various centerbody positions are shown in Fig. 8.

4.2 INLET LOCATION

The location of the inlet relative to the main landing gear has been improved. The gear is longer and is located between the inlets, with the landing gear doors providing a separation plane between the gear and the inlets during gear retraction.

Fig. 9 shows a comparison of inlet-gear relationships on the 733-290 configuration (Phase II-A) and the present 733-390 configuration. Also shown on Fig. 9 is the model configuration which was tested in the low-speed tunnel to evaluate the effect of the landing gear retraction on inlet performance. Fig. 10 shows that satisfactory performance was indicated from the tests.

Landing gear slush deflector tests, using 0.4 scale models, have shown satisfactory progress in developing a gear cover that will eliminate ingestion of foreign objects from the landing gear. Refer to Document D6-19902-1, Aircraft Structures.

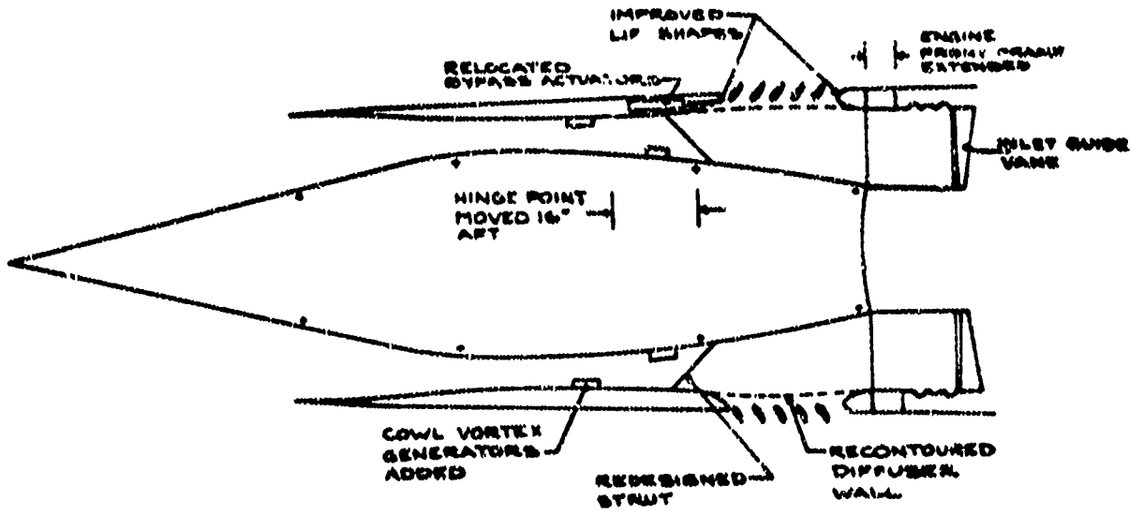

Fig. 7 Inlet Schematic

M_{∞}	M_2	M_1	M_{t2}	M_3	$(P_t/P_t)_2$	60% CONICAL SUPERSONIC DIFFUSER ANGLE — 20 BYPASS DUCT, ENGINE FACE	
2.70	2.55	1.3	.46	.32	.893	6.50°	9.52°
2.55	2.40	1.3	.49	.34	.910	6.40°	7.76°
2.35	2.20	1.3	.55	.36	.918	4.56°	4.92°
2.13	2.00	1.3	.59	.40	.925	4.04°	3.12°
1.91	1.80	1.3	.65	.45	.928	3.56°	1.20°
0~1.90	0~1.79	25~1.3	25~.71	.57~.46	.926~.928		

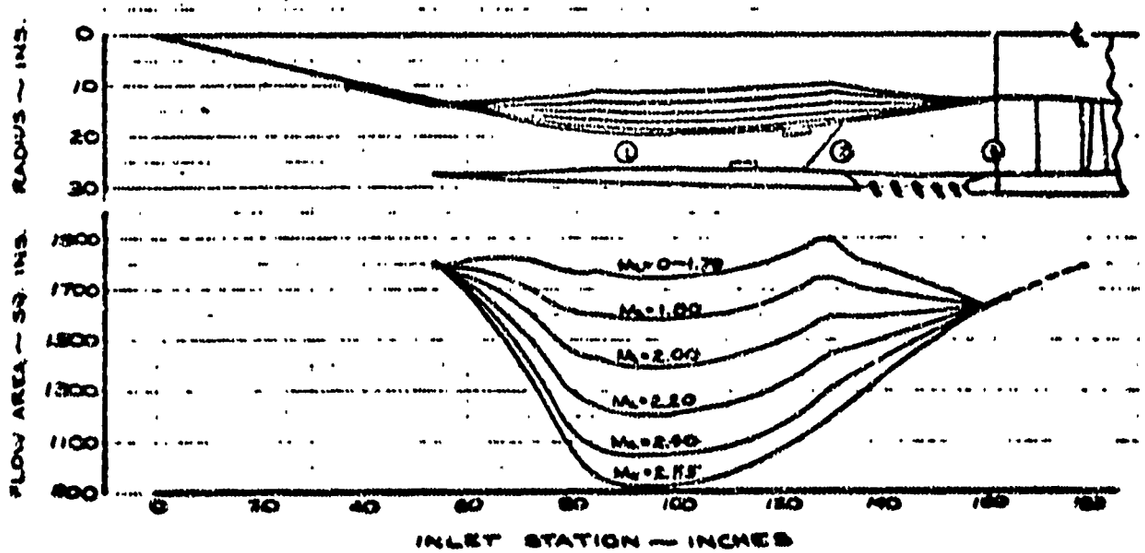

Fig. 8 Inlet Flow Areas and Mach Numbers

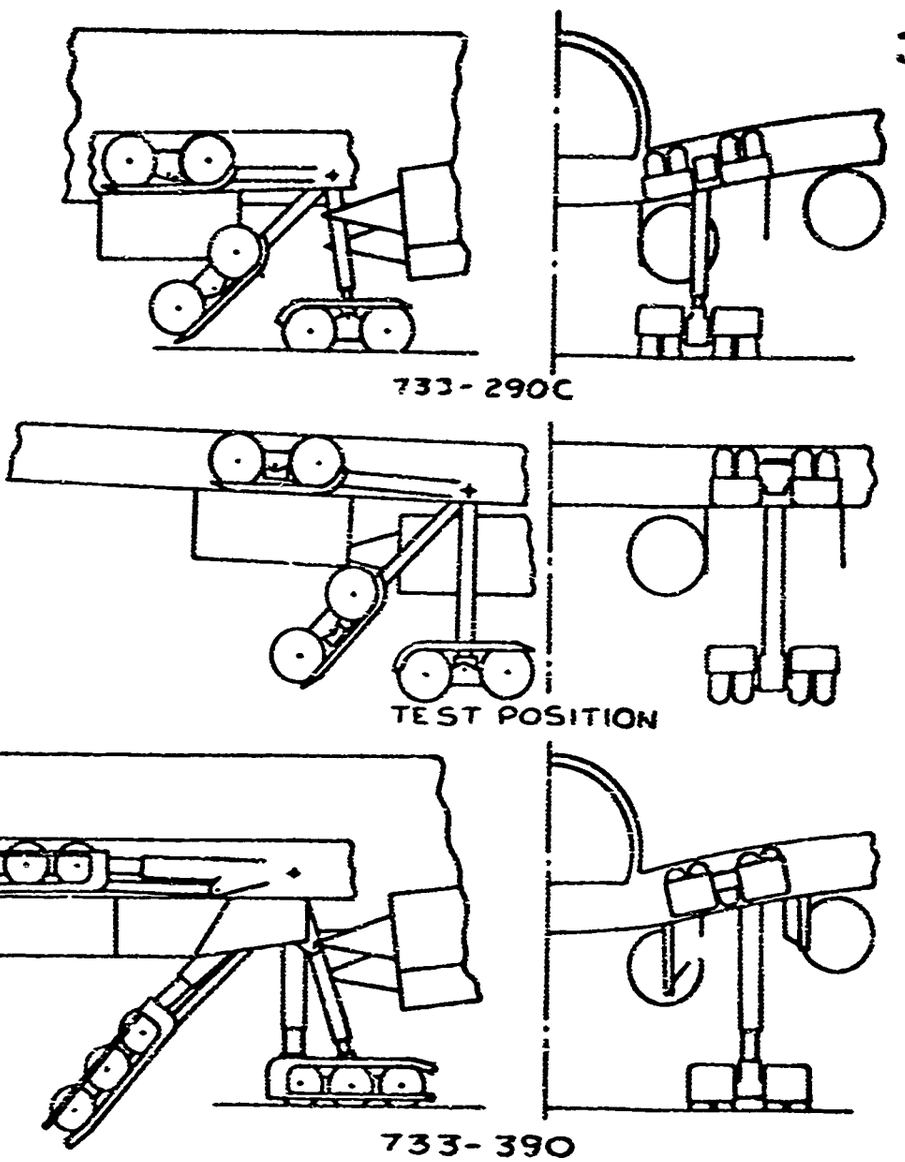

Fig. 9 Inlet-Landing Gear Configurations

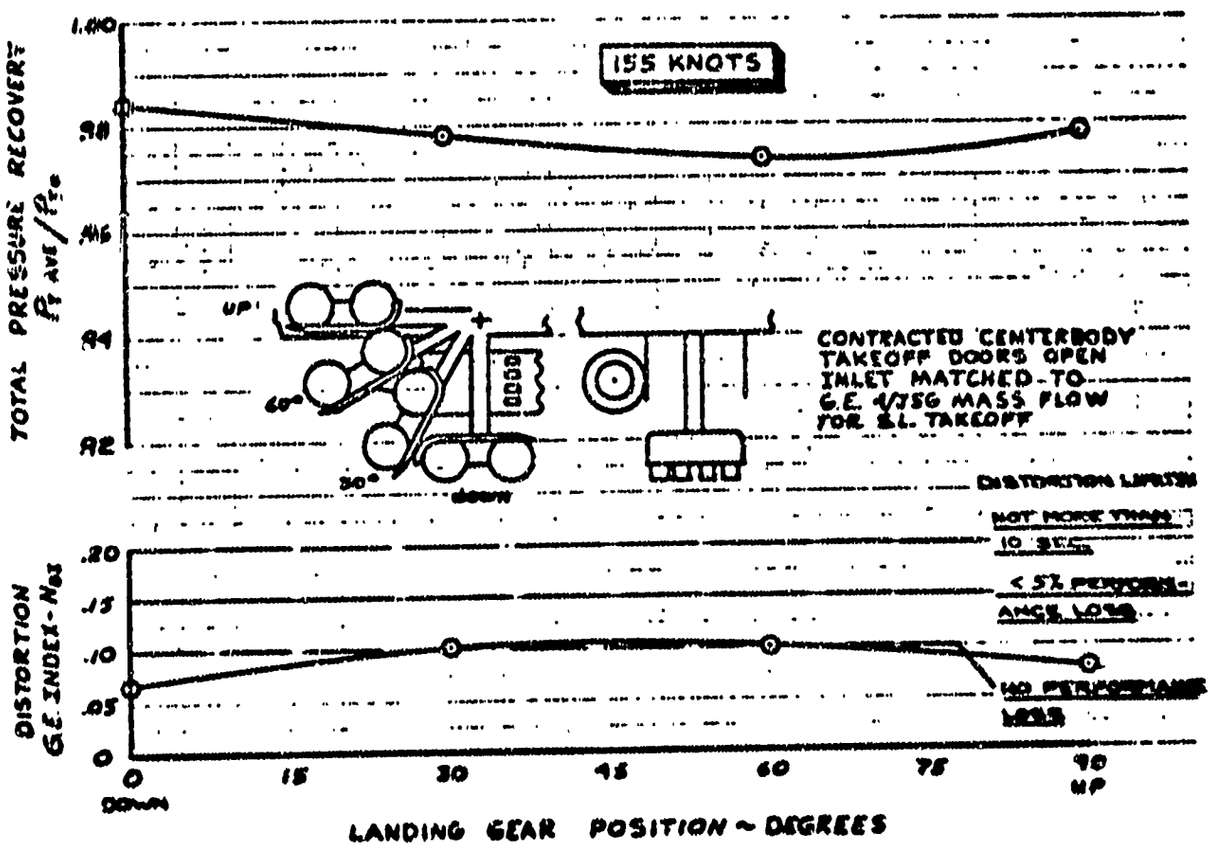

Fig. 10 Inlet Performance During Gear Retraction

4.3 INLET-PRESSURE RECOVERY AND DISTORTION

The inlet recovery schedule used for airplane performance is shown on Fig. 11. This curve is changed from that of Phase II-A to reflect the pressure recovery change that occurs as the inlet switches from the external compression mode to internal compression at an airplane Mach number of 1.9. Some of the data points obtained from small-scale tests which substantiate this performance level are shown.

Compressor face distortion levels obtained by test for various supersonic Mach numbers and with various degrees of supercritical operation are shown in Fig. 12. These levels of distortion have been obtained by the application of vortex generators on the cowl and centerbody and are lower than were available during Phase II-A. The distortion levels are well within the limits specified by General Electric for the engine.

Fig. 12 also shows the distortion levels at inlet angles of incidence for various supercritical margins at cruise conditions.

Extensive testing has been accomplished since Phase II-A to optimize the bleed-hole patterns and vortex generator locations for maximum recovery with minimum bleed and distortion. Fig. 13 summarizes the data obtained from 88 different boundary layer bleed and vortex generator configurations that were tested at Mach 2.5. The last configuration shown on Fig. 13 gave a critical pressure recovery of 91.4 percent, and distortion of 5.4 percent with 5.7 percent bleed. At the normal operating point (2 percent supercritical), the bleed was 5 percent, and the distortion was 4.7 percent.

4.4 INLET MASS FLOW

The inlet mass-flow characteristics obtained by test are presented in Fig. 14. The curves show the ratio of inlet capture flow minus the bleed flow to theoretical lip-area mass flow for various Mach numbers. At a local Mach number of 2.50, the inlet spillage was zero and the bleed flow, as shown, was 5 percent at the design operating point (2 percent supercritical).

4.5 INLET CAPTURE AREA RATIO

The ratio of local stream tube capture area to lip frontal area is shown in Fig. 15. Capture area ratio is based on conical shock spillage, assuming an angle between the centerbody tip and the cowl lip of 27.0 degrees for local Mach numbers between 1.8 to 2.55. As the centerbody contracts, the spike tip moves forward slightly. For the unstarted inlet operation mode, the angle is 26.3 degrees. Between a local Mach number of 1.3 and 1.8, the normal shock is held at the inlet lip and conical shock spillage is based on a lip angle of 26.3 degrees.

The ratio of inlet throat area to lip annulus area is 0.98 when the inlet centerbody is in the unstarted position. The amount of bleed air exiting from the inlet between the cowl lip and inlet throat is assumed to be 1.5 percent of the lip mass flow. The resultant contraction ratio permits control of the normal shock on the lip for

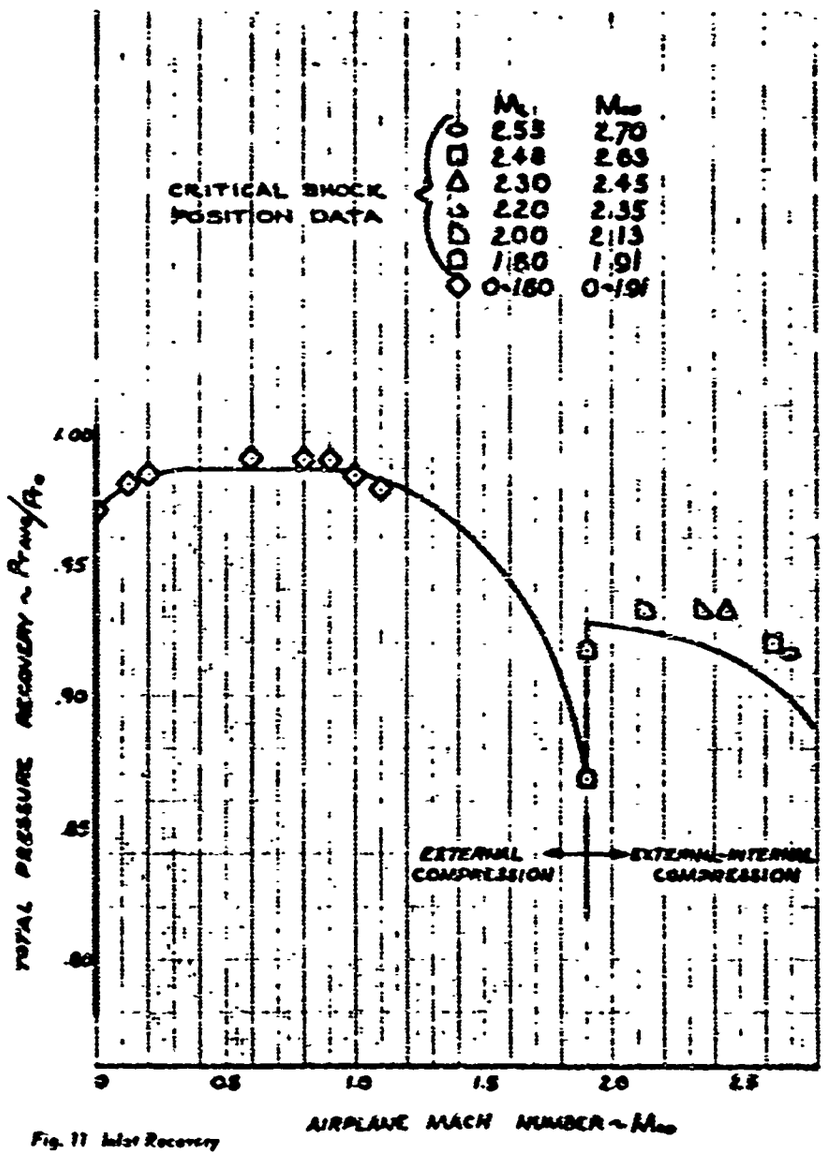

Fig. 11 Inlet Recovery

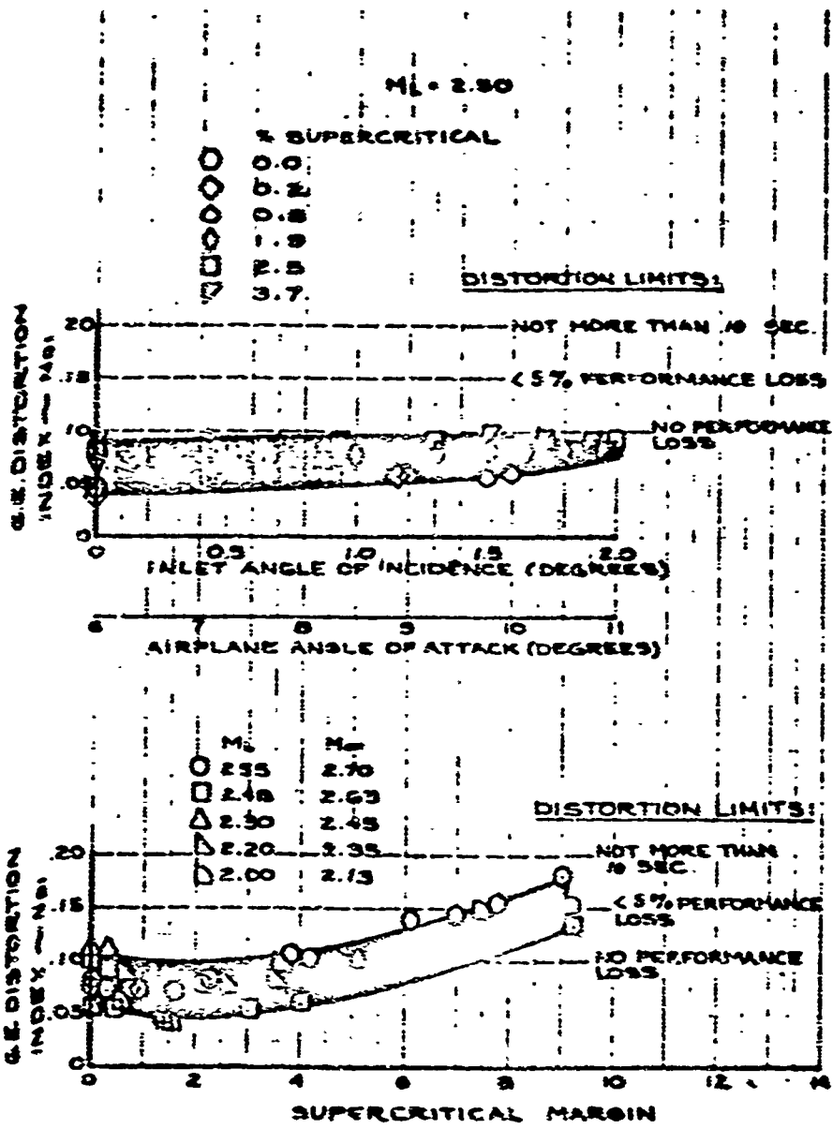

Fig. 12 Inlet Distortion

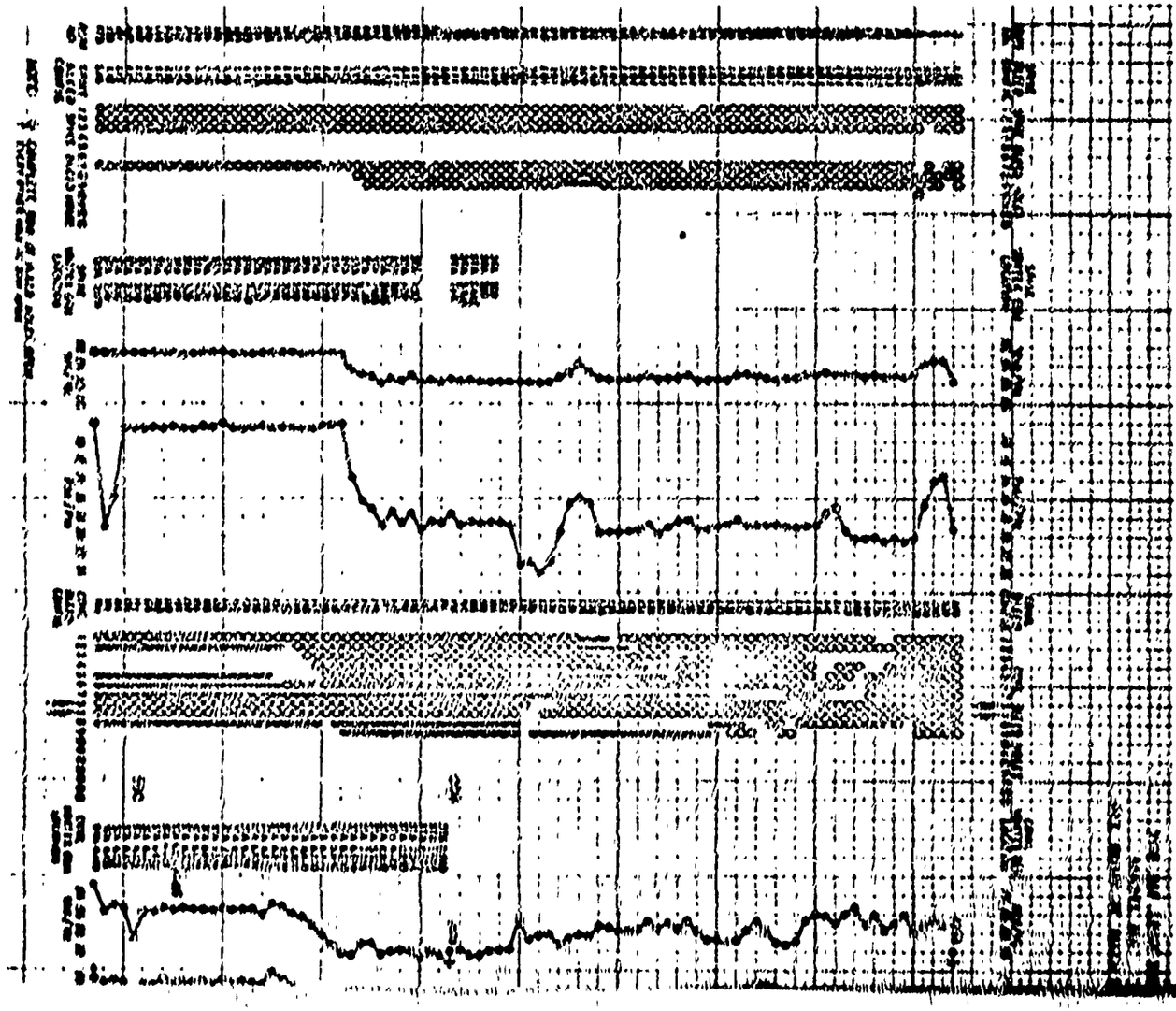

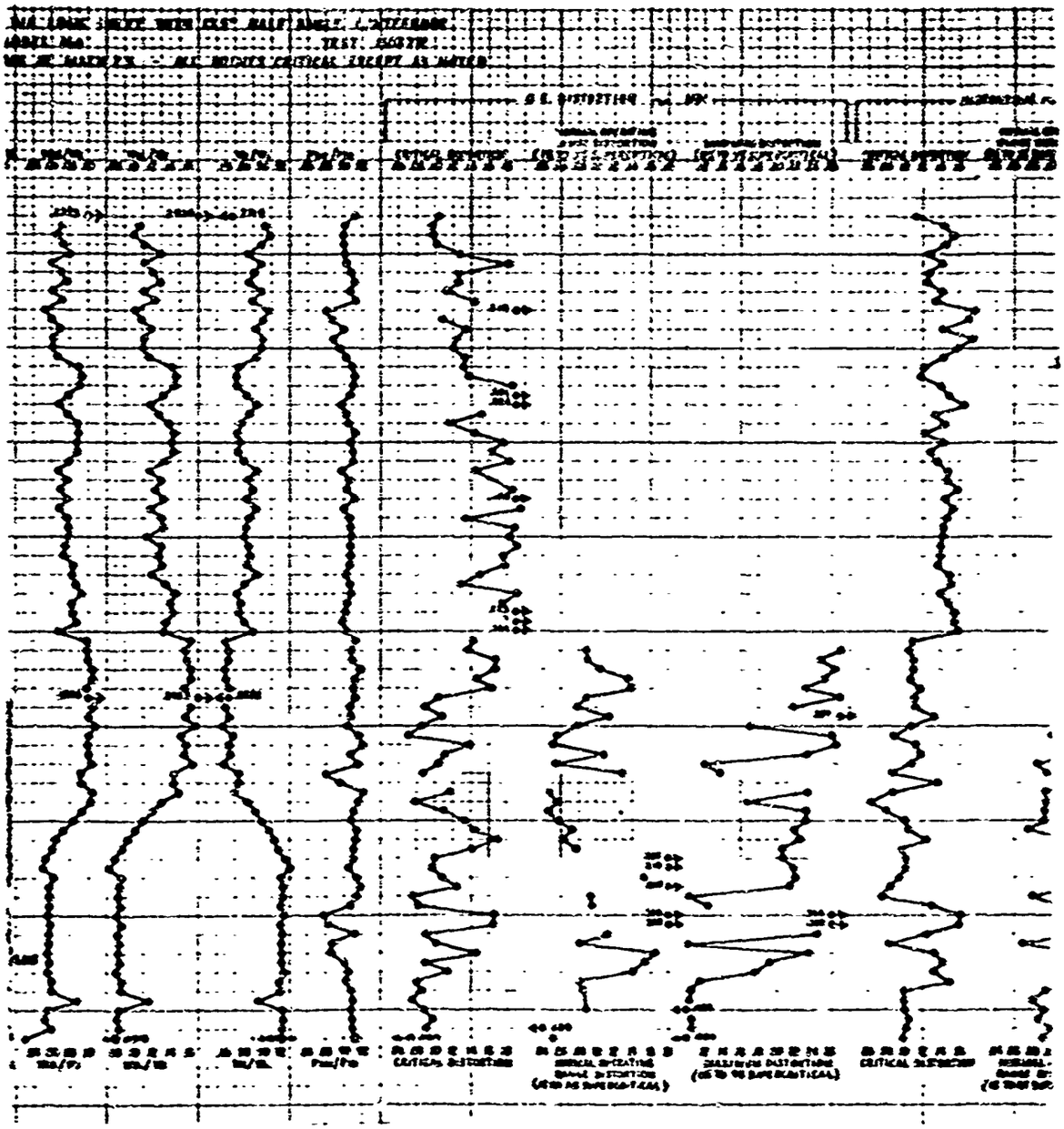

Fig. 13 Inlet Test Data

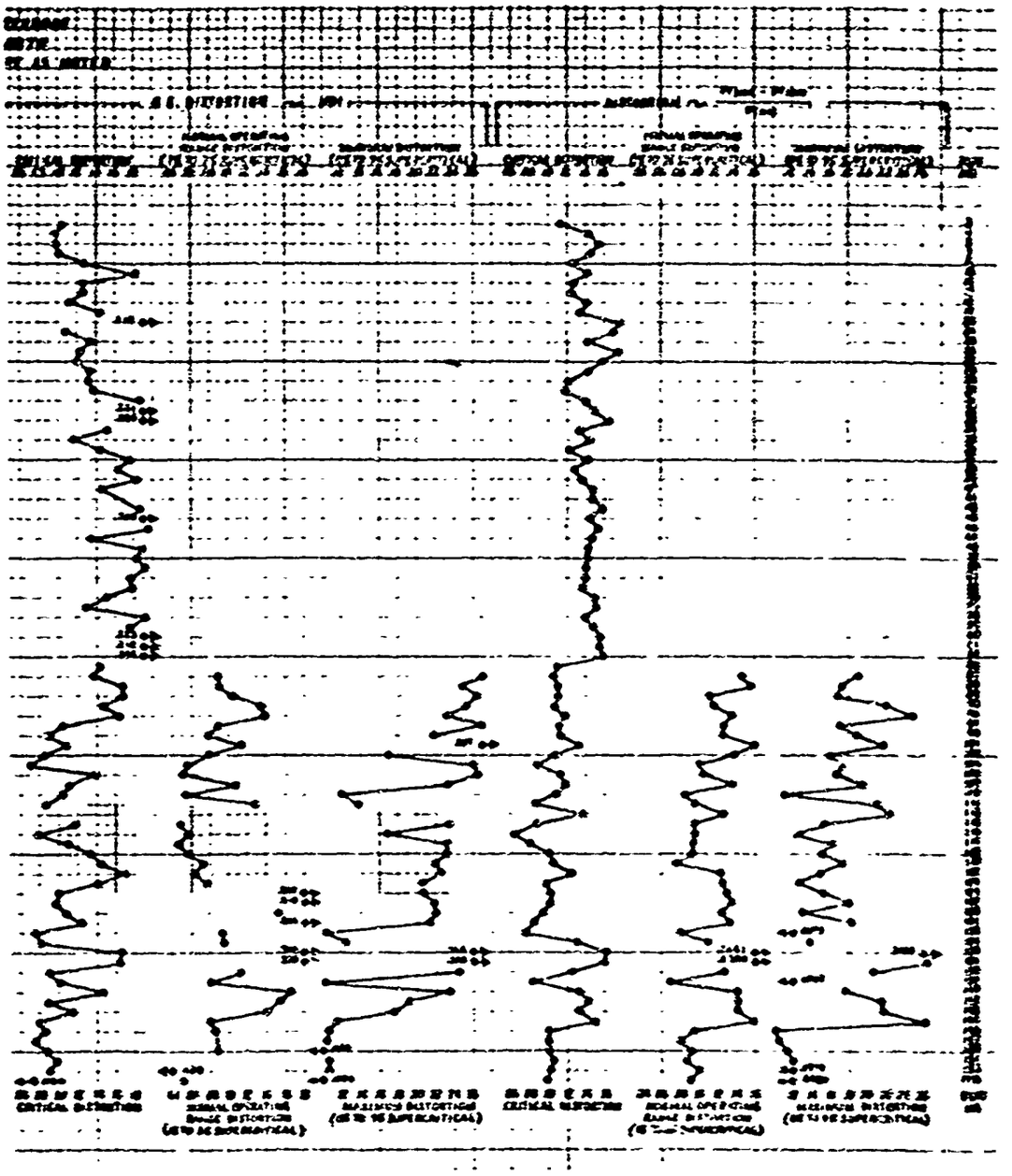

Fig. 13 Inlet Test Data

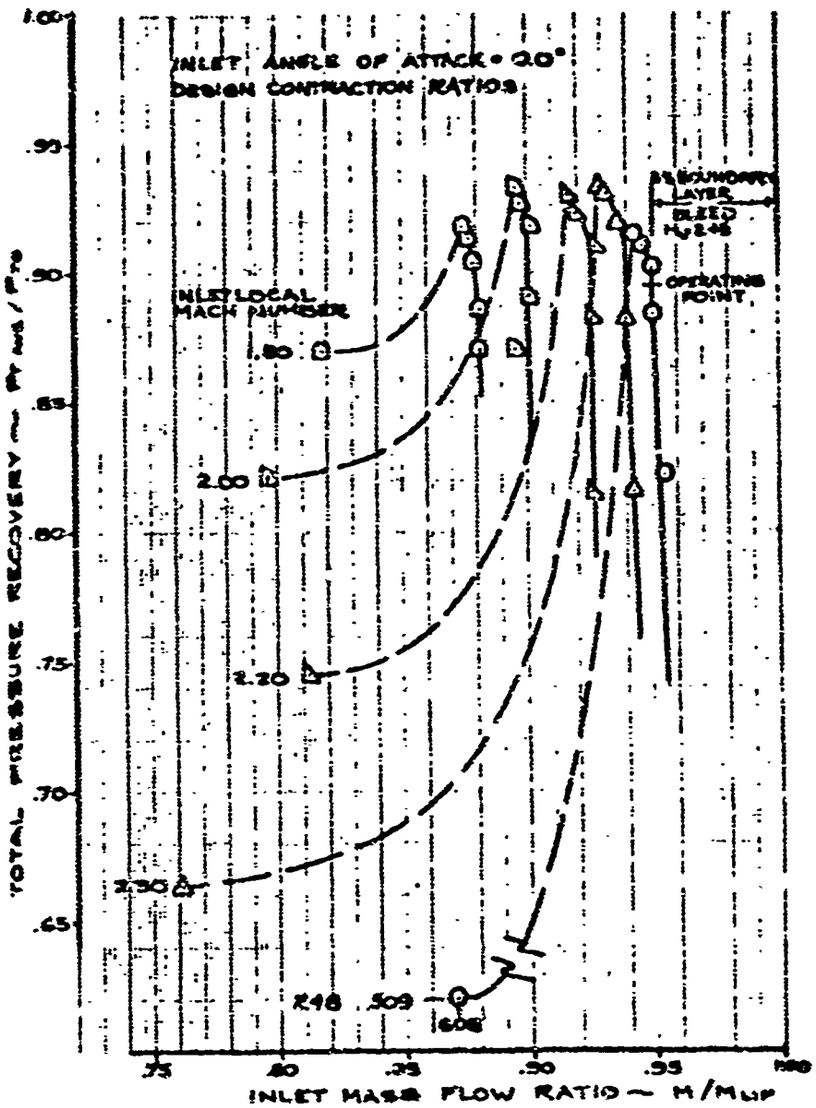

Fig. 14 Inlet Mass Flow Ratios

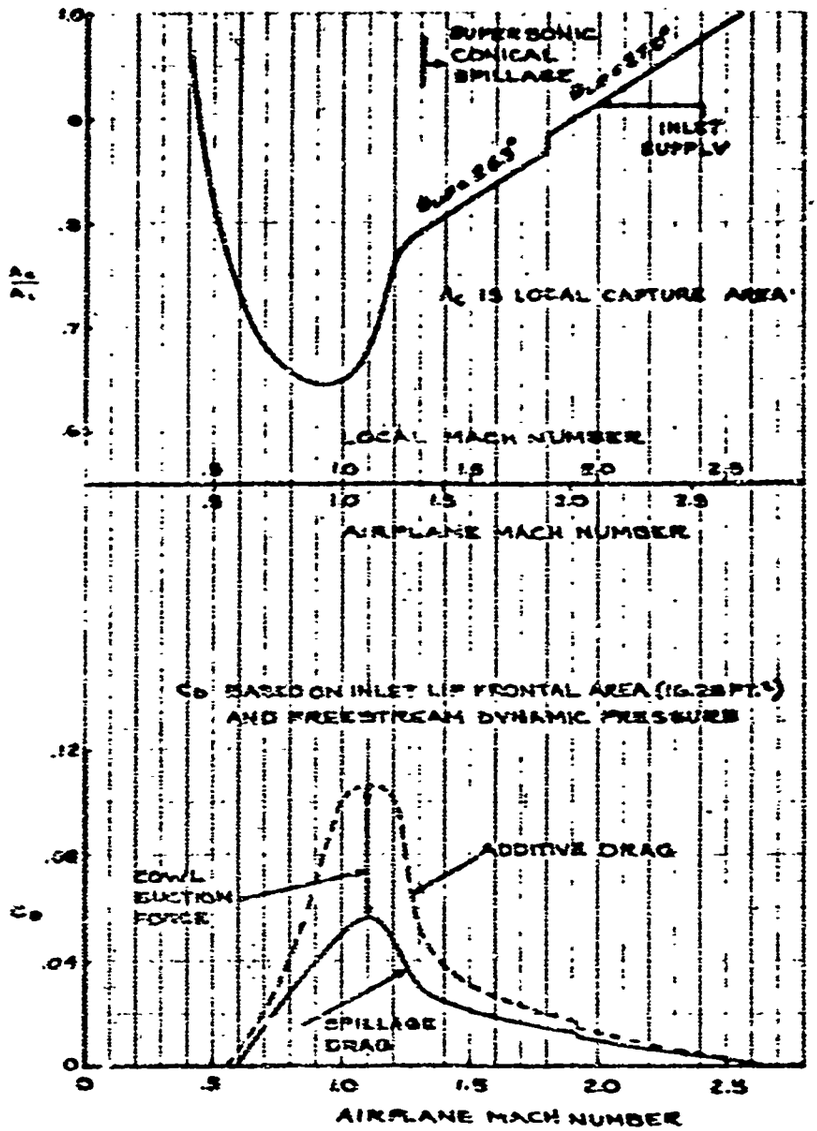

Fig. 15 Inlet Capture Area Ratio and Spillage Drag Coefficient

operations between Mach 1.3 and 1.8. Between Mach 1.0 and 1.3, the normal shock is allowed to move ahead of the lip and increase the amount of external spillage. Below Mach 1.0, all excess air is spilled in front of the inlet.

4.6 INLET ADDITIVE AND SPILLAGE DRAG

Inlet additive and spillage drag coefficients are shown in Fig. 15. Additive drag is defined as the pressure drag caused by streamline turning ahead of the inlet lip. Spillage drag is defined as additive drag minus the change in cowl pressure force (lip section) caused by spillage. Above Mach 1.3, additive drag is computed theoretically using supersonic conical flow theory and the cowl force change due to spillage is computed with the Boeing IBM program 2663M. Below Mach 1.1, additive drags and spillage drags are based on Boeing test data. See Fig. 9-6 through 9-9, Document D6-8680-8, Phase II-A Propulsion Report.

4.7 INLET BLEED DRAG

The assumed inlet centerbody bleed schedule has changed slightly near the inlet starting Mach number because of a better definition of inlet operation at this Mach number. The ratio of bleed-weight flows to inlet-capture-weight flow is shown in Fig. 16. The bleed drag for this bleed schedule is also shown in Fig. 16. Current tests of the bleed system indicate that the values of bleed recovery assumed for drag calculations (0.20 for the centerbody and 0.30 for the cowl) are valid.

4.8 BYPASS SYSTEM DRAG

The inlet supply and engine demand capture area ratios, based on the inlet recovery of Fig. 11, are shown in Fig. 17. The capture area ratio for the bypass air is also shown, as is the average opening angle of the bypass louvers. The bypass capture area ratio (and louver angle) has been increased since Phase II-A in the range of $M_{local} = 1.4$ to 1.8. This is due to the change in inlet recovery at these speeds. Consequently, the bypass drag coefficient, which has been increased, is shown in Fig. 17.

4.9 IDLE-DESCENT EXCESS AIR DRAG

During idle-descent, reduced engine-mass flow causes increased excess air drag. A composite inlet supply-engine demand curve and the resultant drag coefficient are shown in Fig. 18. The increase in engine demand at Mach 1.3 is caused by the engine control change from low idle rpm to normal idle. From Mach 1.9 to Mach 2.7, the excess mass flow is bypassed. Below Mach 1.9, a portion of the excess air is spilled between the normal shock and the lip, and the remainder is bypassed.

4.10 FULL-SCALE TEST INLET CENTERBODY

Fig. 19 is an assembly drawing of the variable-diameter inlet centerbody which is being designed and fabricated from titanium alloys for test evaluation. Design releases are approximately 95 percent complete. Scheduled completion of the centerbody is March 31, 1966.

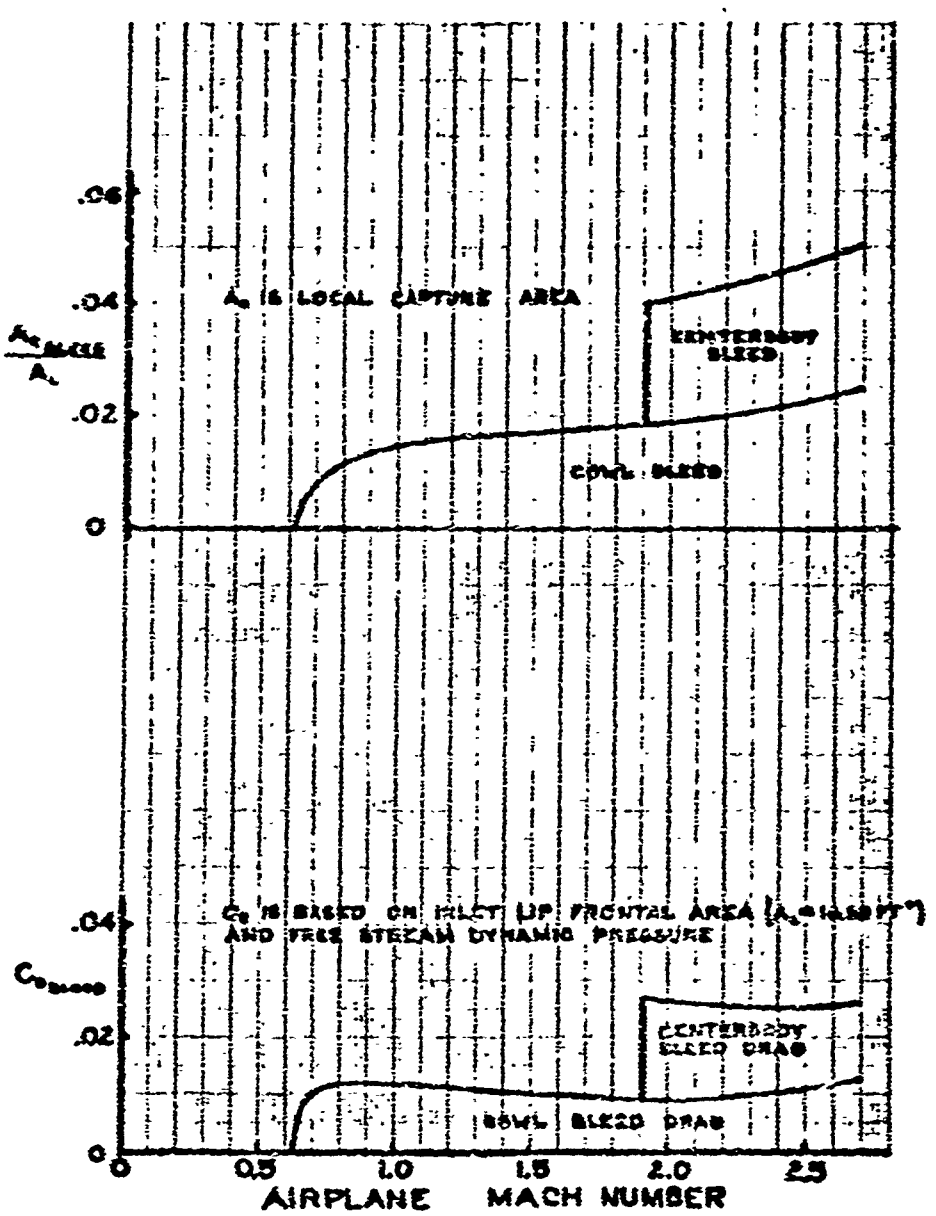

Fig. 16 Inlet Bleed Capture Area Ratio and Bleed Drag Coefficient

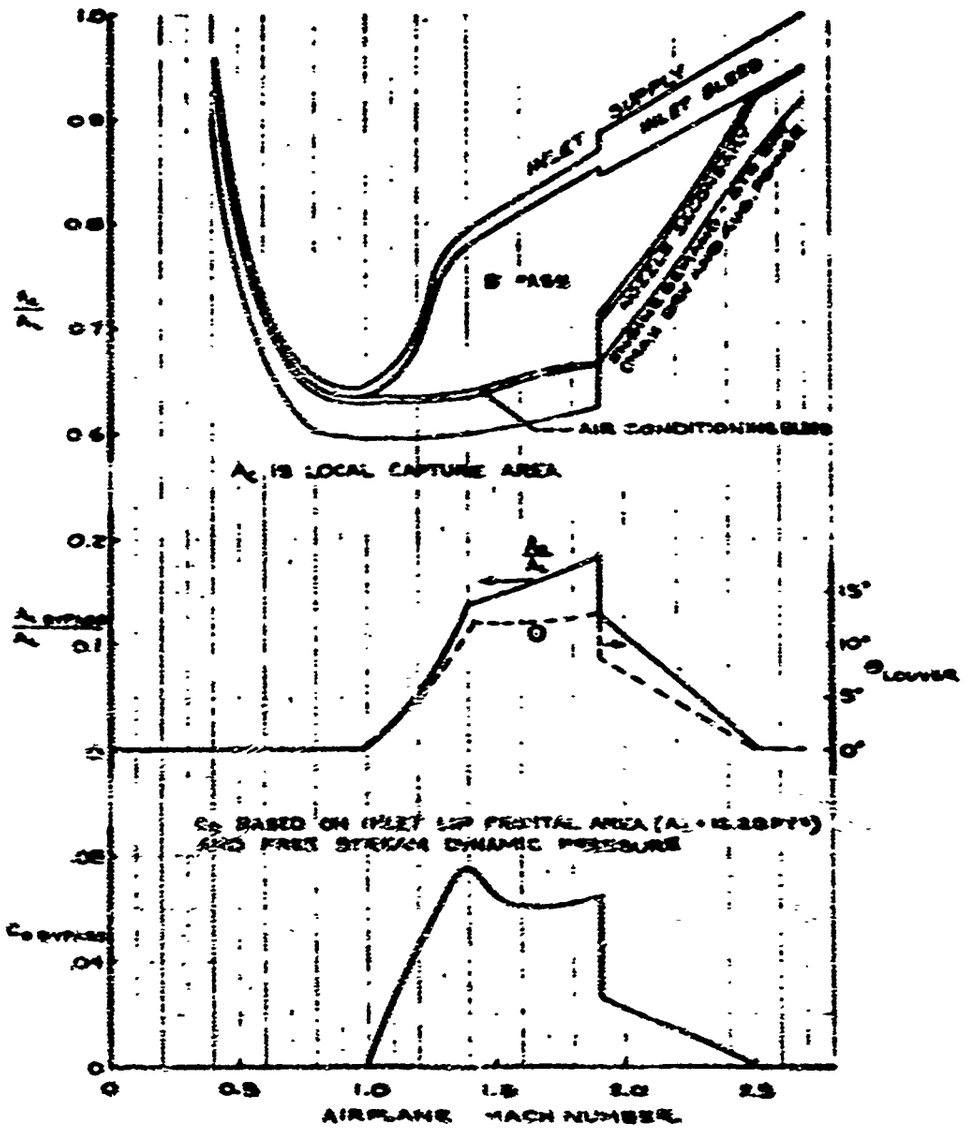

Fig. 17 Bypass Capture Area Ratio and Bypass Drag Coefficient

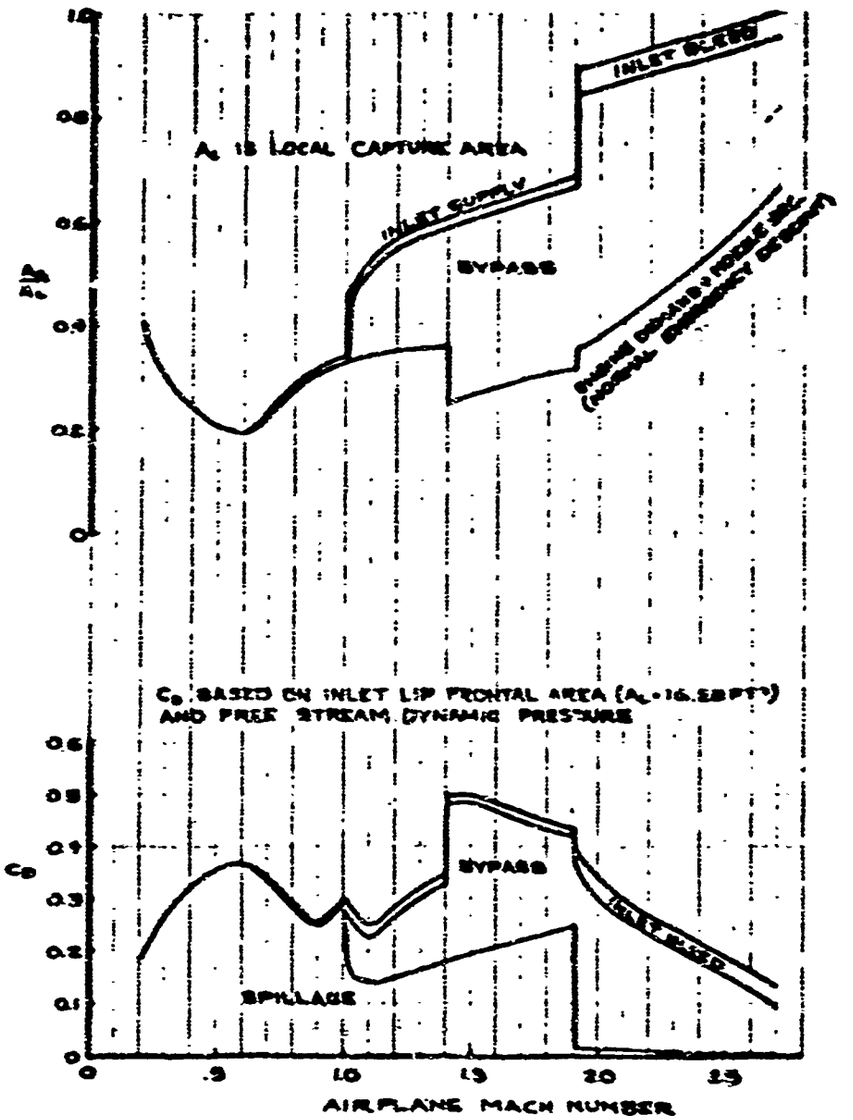

Fig. 19 Idle Descent Capture Area Ratio and Drag Coefficient

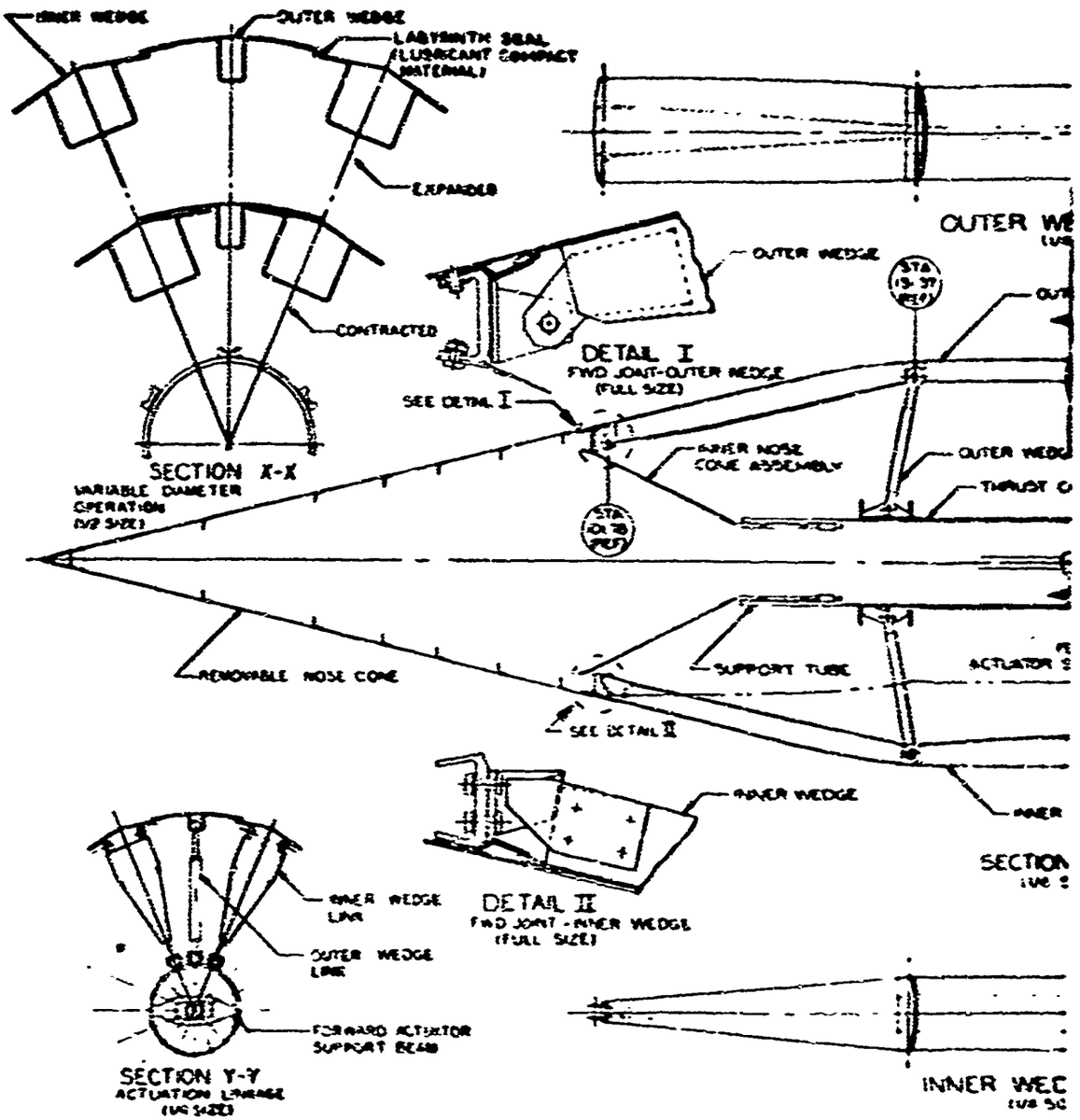
INNER WEDGE
OUTER WEDGE
LABYRINTH SEAL (LUBRICANT COMPACT MATERIAL)
EXPANDER
CONTRACTED
SECTION X-X
VARIABLE DIAMETER OPERATION (1/2 SIZE)
OUTER WEDGE
DETAIL I
FWD JOINT-OUTER WEDGE (FULL SIZE)
SEE DETAIL I
INNER NOSE CONE ASSEMBLY
OUTER WEDGE
THRUST
REMOVABLE NOSE CONE
SUPPORT TUBE
ACTUATOR
SEE DETAIL II
INNER WEDGE
INNER
DETAIL II
FWD JOINT - INNER WEDGE (FULL SIZE)
INNER WEDGE LINK
OUTER WEDGE LINK
FORWARD ACTUATOR SUPPORT BEAM
SECTION Y-Y
ACTUATION LINKAGE (1/8 SIZE)
OUTER WE
INNER WEC

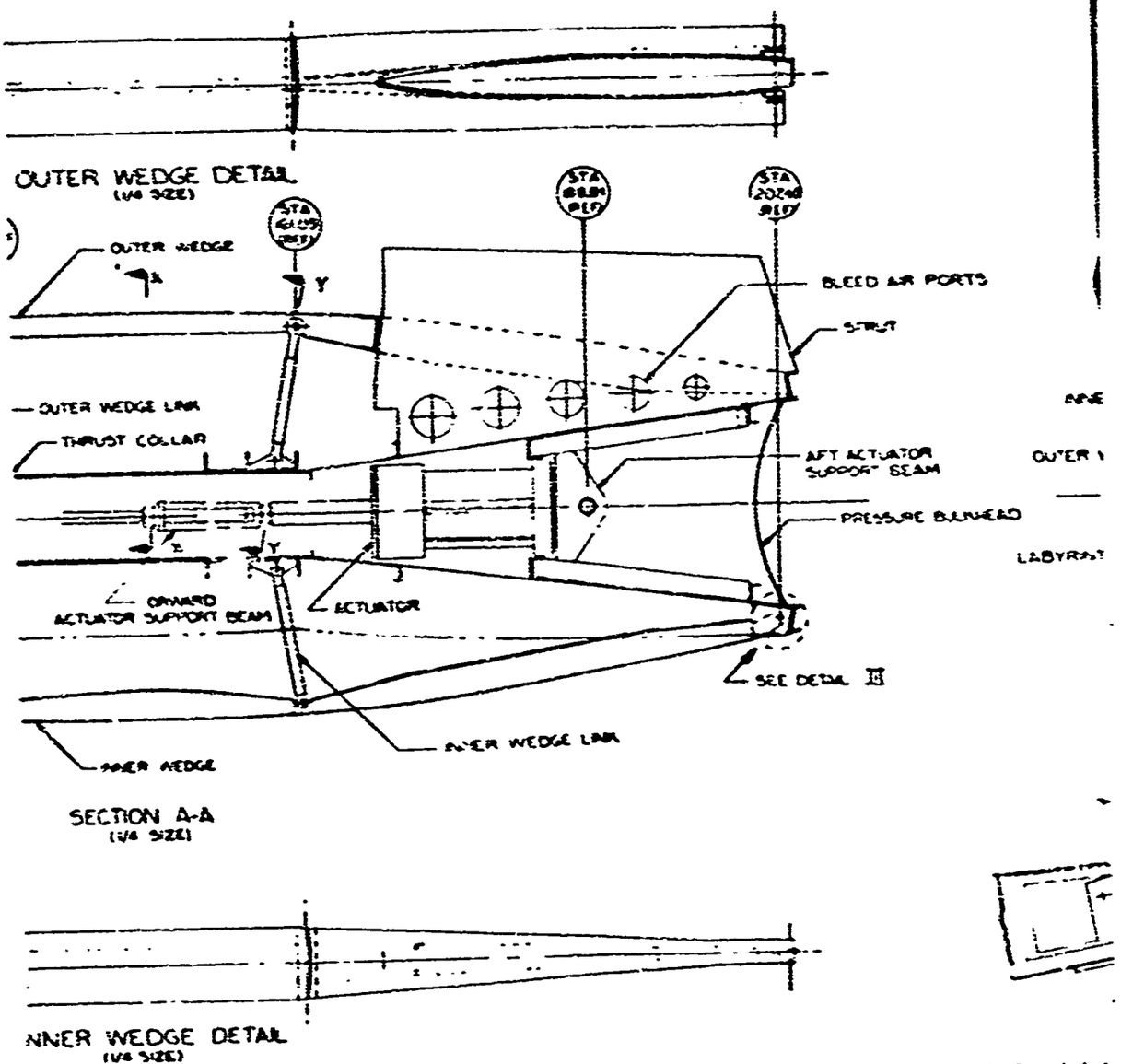

Fig 19 Inlet Countrbody A

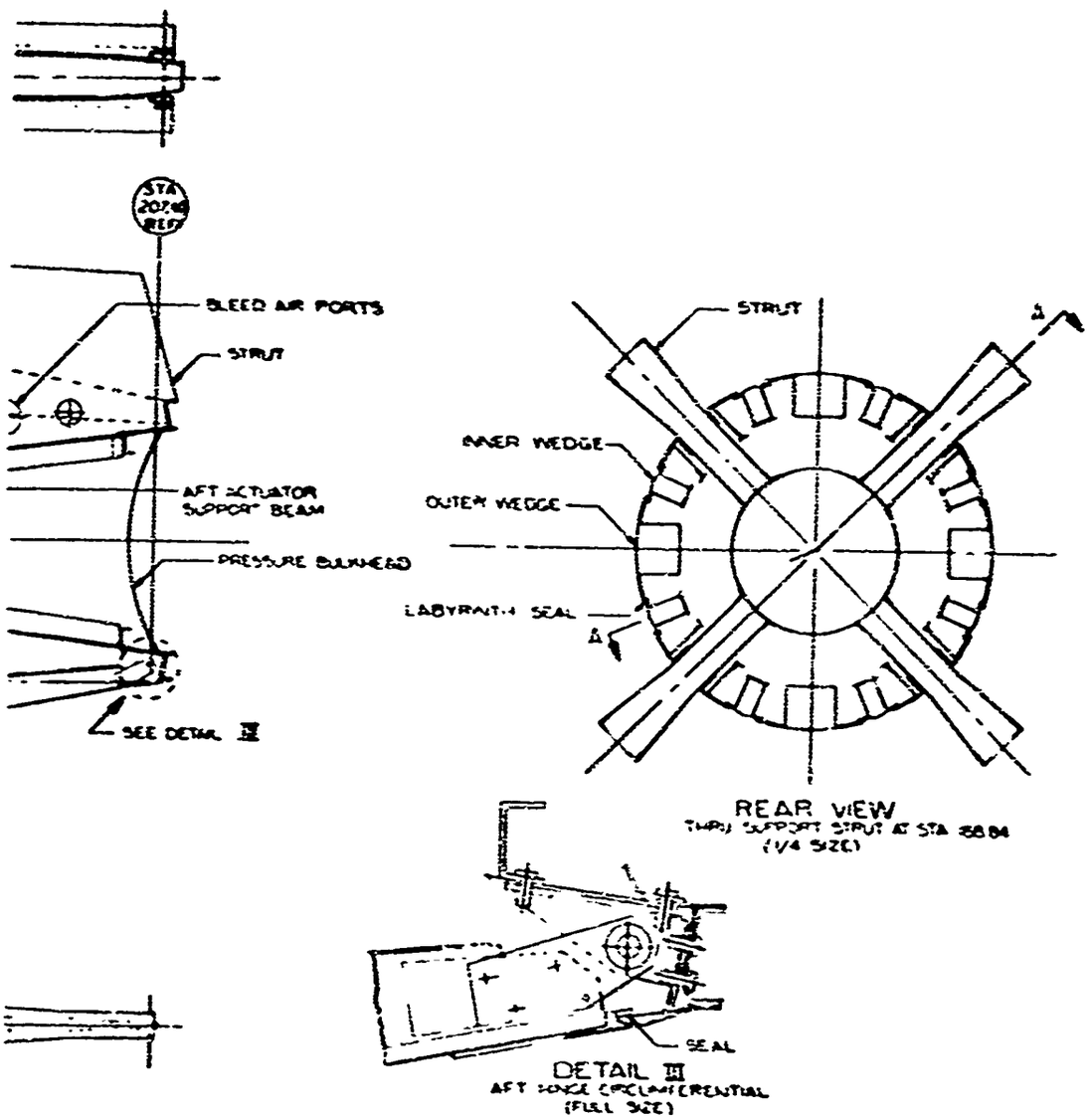

Fig. 19 Inlet Centerbody Assembly – Full Scale Test

The scale of the test centerbody is full size for an inlet designed for the General Electric GE4/J5C 475 pounds-per-second airflow engine. Pressure and temperature design environment is consistent with the 733-390 airplane flight placard.

The application of value engineering techniques to obtain a mechanism that is lower in cost, more efficient, and simpler has resulted in several detail changes to the design of the test centerbody.

The hardware design necessitates hogged-out, machined parts where forgings or castings would be more appropriate for a production run. Essentially production manufacturing methods are being used to form sheet-metal components. A record is being kept of tool concepts and fabrication procedures used.

5.0 AIR-INDUCTION CONTROL SYSTEM

The differences between the previous and the present control system consist of a redesign of the normal shock position indicator system for flight deck display, change of pressure locations for restart sensor, and installation of a buzz warning light. A simplified block diagram of the inlet control system is shown in Fig. 20. A schematic diagram of the complete inlet control system is included in Ref. 3.

Since Phase II-A, wind-tunnel testing has been conducted to substantiate the use of constant control signals with aerodynamic feedback. Calculations for the steady state and transient accuracy were made for the proposed centerbody and normal shock control loops for a number of selected conditions (see Par. 5.5).

5.1 NORMAL SHOCK POSITION INDICATION

The redesigned system has been made independent of the bypass door control and consequently will function to indicate the normal shock position during both automatic and manual control of the inlet. A block diagram is shown in Fig. 21.

The system determines the stability margin of the inlet by comparing the measured pressure recovery with the computed critical inlet recovery. Test results on a representative inlet show that the critical inlet recovery varies with local inlet mach number and centerbody radius, as shown in Fig. 21. These curves can be represented and computation of critical inlet recovery accomplished by the use of a simple, compact, analog function generator. The critical inlet recovery thus computed and the inlet recovery measured at the compressor face will be compared and the difference displayed on the instrument panel. An error analysis will be conducted to determine the system accuracy.

5.2 PRESSURE LOCATIONS FOR RESTART SENSORS

As shown in Fig. 20, the pressure signal pickups for the restart sensor are the cowl lip static (p_{cl}) and centerbody tip total (P_{SO}). The pressure signals generated by these probes are shown on Fig. 22. Whenever the inlet is started, the measured ratio $\frac{(P_{cl})}{(P_{SO})}$ is below the reference value, and whenever the inlet is unstarted, the ratio is above the reference value. This change was made to obtain pressure signals that positively indicate inlet operation at all Mach numbers.

5.3 BUZZ AND UNSTART WARNING LIGHT

The buzz and unstart warning light has been added to the flight deck display panel and is located just above the shock position indicator.

The buzz and unstart signal is obtained from a pressure switch that uses the restart sensor pressure signals to cause the light on the display panel to be on whenever the inlet is unstarted. Pressure pulsations that occur during buzz will cause this same light to switch

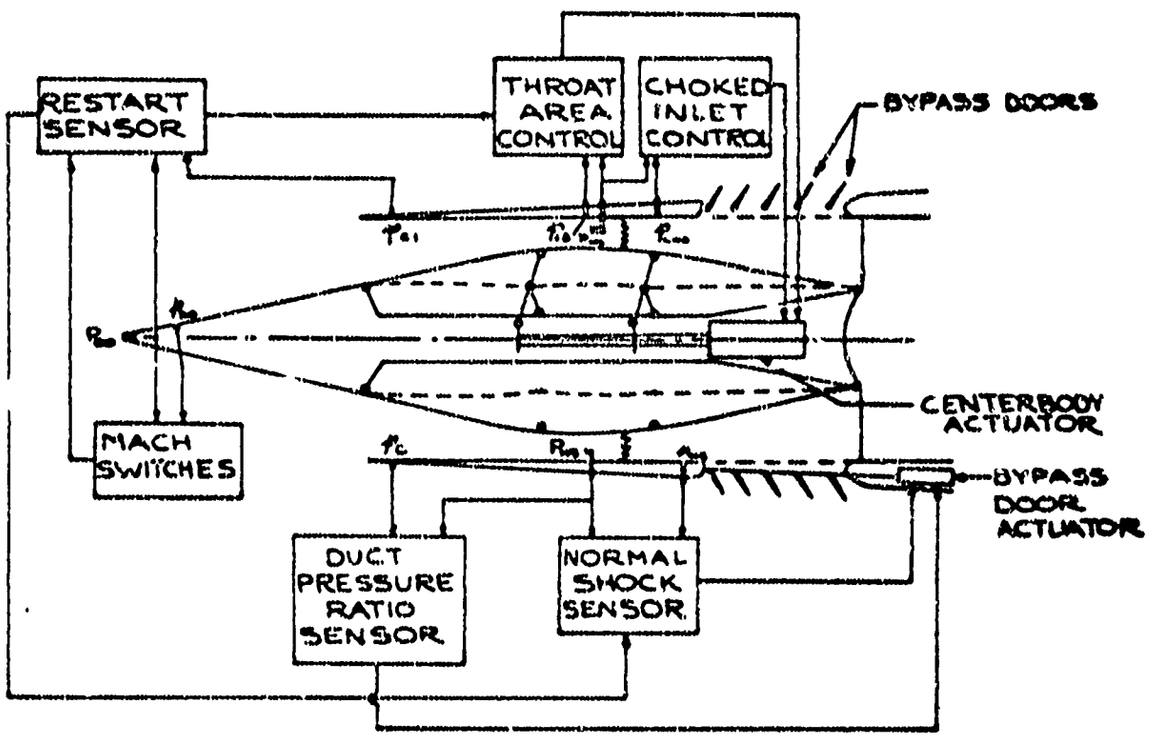

Fig. 20 Inlet Control Block Diagram

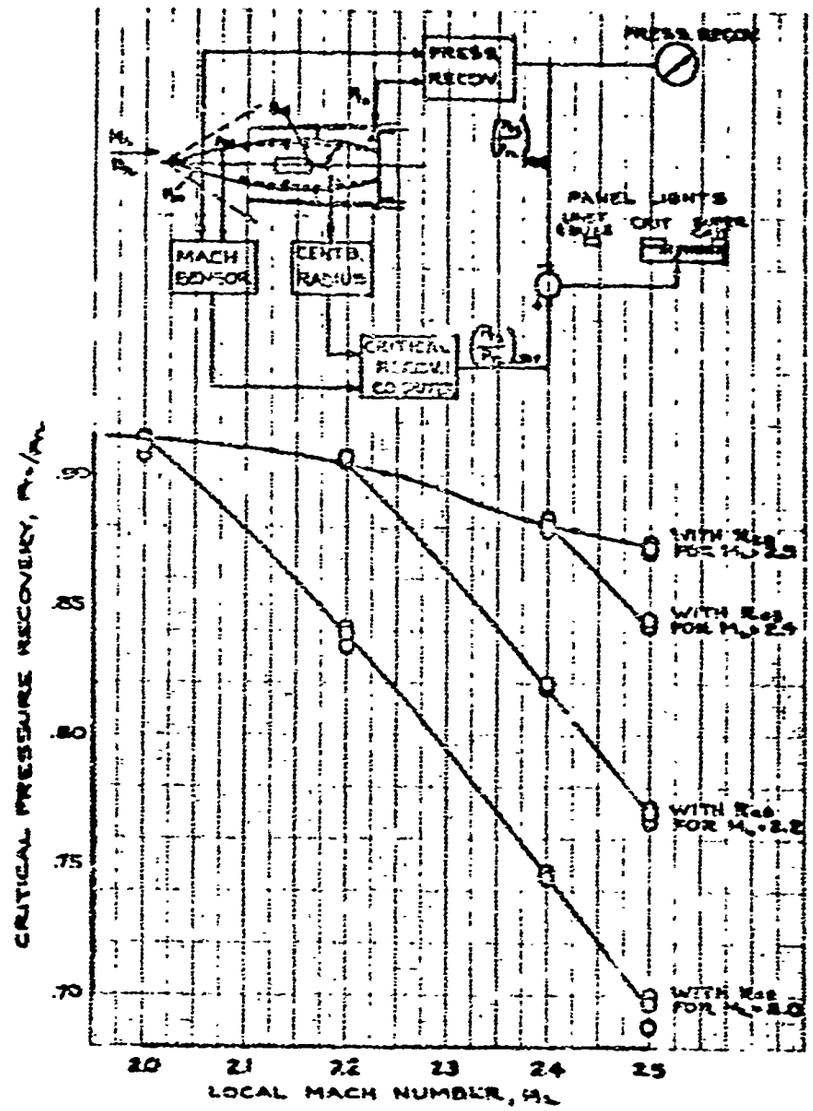

Fig. 21 Normal Shock Position Display and Conical Inlet Recovery

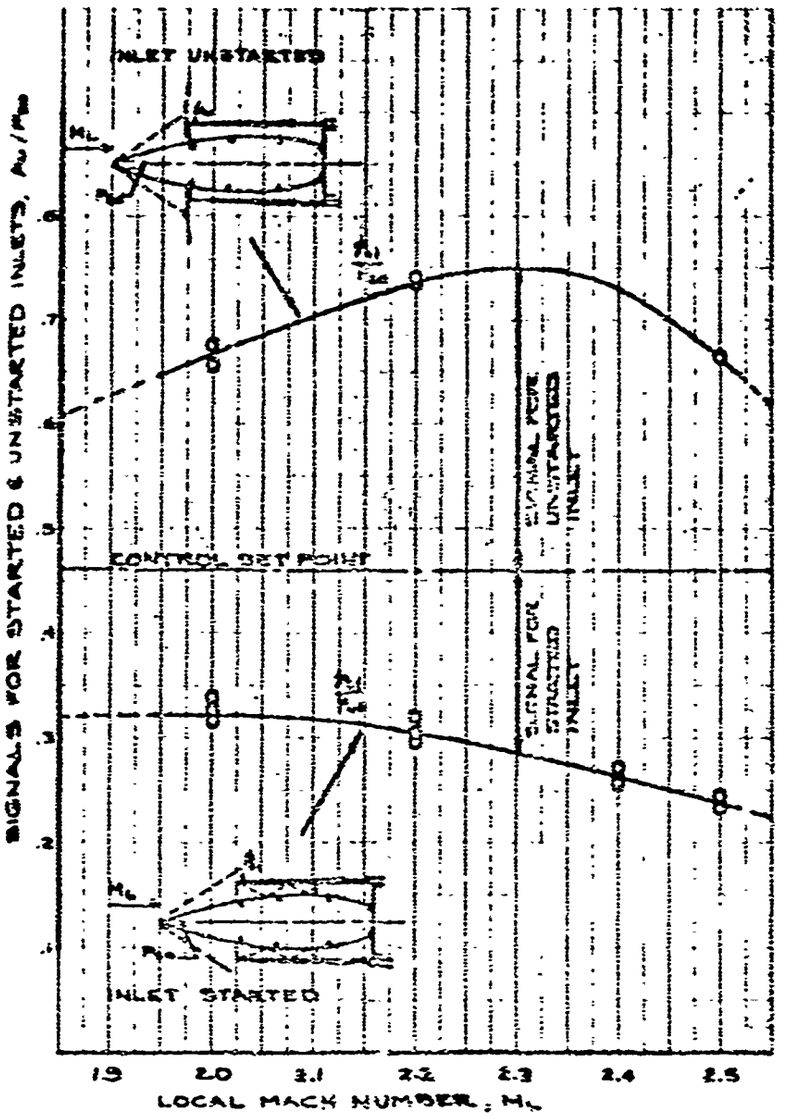

Fig. 22 Restart Control Signal Characteristics

on and off intermittently to produce a visual display on the panel of the shock pulsations occurring during buzz. When buzz is terminated by the buzz suppressor (which puts the inlet in a safe, stable, unstarted position), the light will remain on to designate an unstarted inlet. The unstart warning light will be deactivated whenever the airplane Mach number is below 1.9.

5.4 INLET CONTROL SIGNAL TESTS

The pressure signals selected for the centerbody control during the mixed compression mode of inlet operation are the total and static pressures immediately upstream of the throat (P_{TIS} and p_{cb}, Fig. 20) and those for the normal shock control are the same total pressure and the subsonic diffuser static pressure (P_{TIS} and p_{DIS}). An extensive series of tests was conducted to verify theoretically predicted signal characteristics. These are discussed below.

5.4.1 CENTERBODY RADIUS CONTROL

The selection of the throat static and total pressure for the centerbody control is based on the theory that the static-to-total pressure ratio in a supersonic stream is a function of Mach number. Since the throat Mach number is kept at approximately 1.3 throughout the mixed compression mode, the use of a constant centerbody control signal and an aerodynamic feedback in the centerbody control loop is justified.

Results of tests to ascertain the variation of the control pressure ratio as functions of the inlet Mach number and of the centerbody radius are shown in Fig. 23. A control set point for the model test throat Mach number of 1.35 intersects with the sensing signals, as shown.

The points of intersection occur at the proper centerbody radius for the inlet Mach numbers investigated. These data verify that a constant control sensor pressure ratio will position the centerbody to the proper radius at all Mach numbers.

The generation of an inlet angle-of-incidence bias signal for the centerbody control, by using more than one static pressure tap around the throat annulus, was tested. It was found that four static pressure positions, 90 degrees apart in the annulus, could sense an incidence angle change of 0.25 degree. The system requires a pressure selector capable of selecting the highest of the static pressures for the control signal. Current fluid valve technology can provide a selector of the required sensitivity (2 percent pressure differential).

5.4.2 NORMAL SHOCK (BYPASS DOOR) CONTROL

Several locations in the subsonic section of the inlet were experimentally examined to find a suitable static pressure signal which, when referenced to the throat total pressure, would control the normal shock during the mixed compression mode.

A satisfactory static location was found as indicated by the test results shown in Fig. 24. When a control set point of 0.65 is selected, the curves intersect at the desired value for stable, efficient inlet operation, which is 2 percent supercritical.

Satisfactory centerbody and bypass door control signals in small scale inlet configurations have been found; consequently, it is believed that similar control pressure signals can be found for the full-scale inlet. Wind-tunnel tests with an 11-inch variable geometry inlet model and actual control hardware will be accomplished during Phase II-C to confirm the suitability of these control signals.

5.5 STEADY-STATE AND TRANSIENT CONTROL ACCURACY

Preliminary calculations were carried out to estimate the steady-state and transient accuracy of the centerbody and bypass door control loops at a number of inlet Mach numbers. The results for Mach 2.7 and 65,000-foot altitude are presented in Table B.

For these calculations, error data for the pilot valve breakaway force were obtained from control system vendors. The transient errors were obtained from the results of mathematical simulation of the inlet and control system models.

The transient error of the centerbody control was based on a Mach number change of 0.05 in 0.02 second, and the bypass door control error was based on an engine corrected airflow change of 5 percent in 0.25 second.

The current calculations indicate that the accuracy of both control loops is acceptable for all mixed compression operation. This analysis will be expanded to include all elements of the inlet system during Phase II-C.

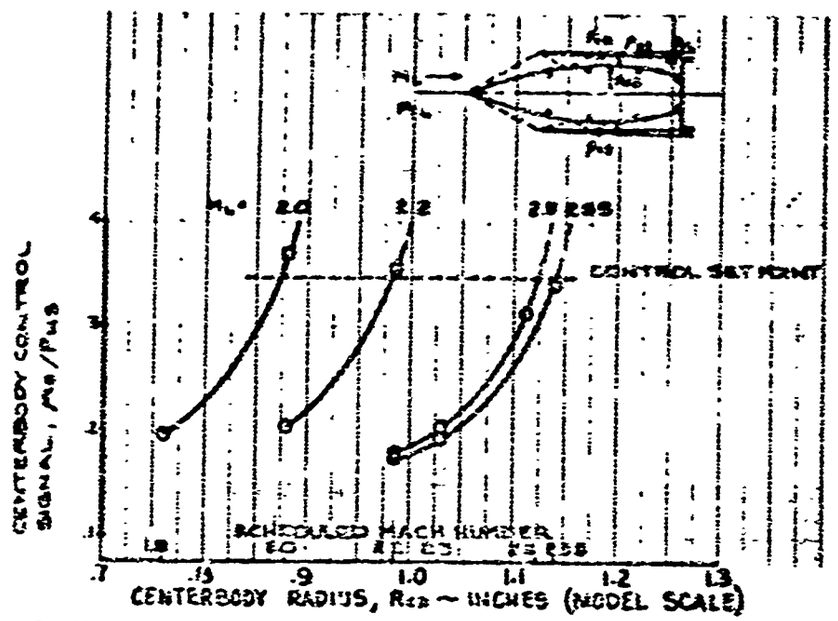

Fig. 23 Centerbody Control Signal Characteristics

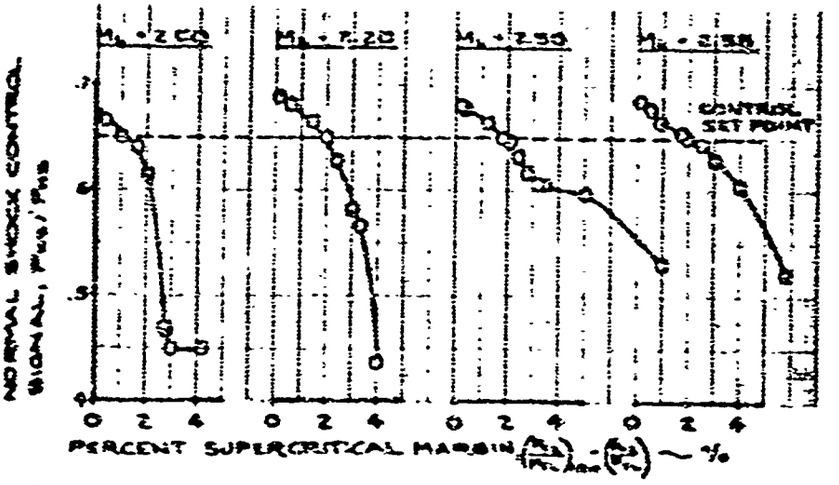

Fig. 24 Normal Shock Control Signal Characteristics

Table 8 Steady-State and Transient Control Accuracy at $M_{00} = 2.70$ and 65,000 Feet

	CENTERBODY CONTROL LOOP			BYPASS DOOR CONTROL LOOP		
	SOURCE OF ERROR	ERROR: CENTERBODY RADIUS (In.)	ERROR: THROAT MACH NO.	SOURCE OF ERROR	ERROR: BYPASS AREA ($In.^2$)	ERROR: INLET RECOVERY (%)
STEADY STATE	THROAT MACH SENSOR	±0.0135	±0.007	NORMAL SHOCK SENSOR	±0.15	±0.05*
TRANSIENT	CENTERBODY CONTROL SYSTEM	±0.3287	±0.090	BYPASS DOOR CONTROL SYSTEM	±5.01	±0.381

6.0 ENGINE CONTROL SYSTEMS

The following improvements have been made to the engine control systems:

- The thrust lever quadrant and reverser operation has been simplified by the tentative elimination of the null thrust reverser position.
- The low-idle position of the start lever is separated from the flight shutdown position by a positive detent to prevent inadvertent shutdown of the engine when low-idle fuel flow is selected at the start of descent.
- The normal idle setting of the thrust lever (61 percent rpm) is separated from the low-idle position (50 percent rpm) by a positive detent. The low-idle position may be used during descent and ground taxi. Normal idle (61 percent) is used during landing approach to provide rapid engine acceleration for go-around.
- Operation with the exhaust nozzle open and inlet choked for noise abatement during the power cutback period after takeoff is now included in the engine control system.
- Engine airflow trim during nonstandard days has been revised to include the capability of trimming the engine to match the inlet for hot days as well as cold days. Modulation of the nozzle secondary air control valve is used to pass more air through the cowl cavity to the nozzle on hot days. This improves the hot-day range capability of the airplane and increases the flexibility of trimming for engine and inlet tolerances.

Additional information on the engine controls and their requirements is available in Ref. 4.

6.1 THRUST-LEVER QUADRANT

The revised thrust-lever quadrant is shown in Fig. 25. The null thrust mode has been tentatively eliminated to simplify thrust-reverser operation and controls. Idle rpm has been increased to 61 percent during approach to provide good engine acceleration time. Additional studies are required to finalize this system.

6.2 NOISE-ABATEMENT CONTROL

During landing approach and after power cutback on takeoff, the noise abatement control selector, which is manually operated, provides choked inlet operation and full-open nozzle position. This feature reduces airport and community noise during airplane operation.

The choked inlet control is the same as that in Phase II-A. The revised nozzle-area schedule for takeoff and landing operation is shown on Fig. 26. This schedule provides the required thrust levels during cutback after takeoff and during landing approach with the nozzle full open. Thus, engine noise is minimized by lowering the specific thrust (thrust/unit airflow) for a given thrust level. The

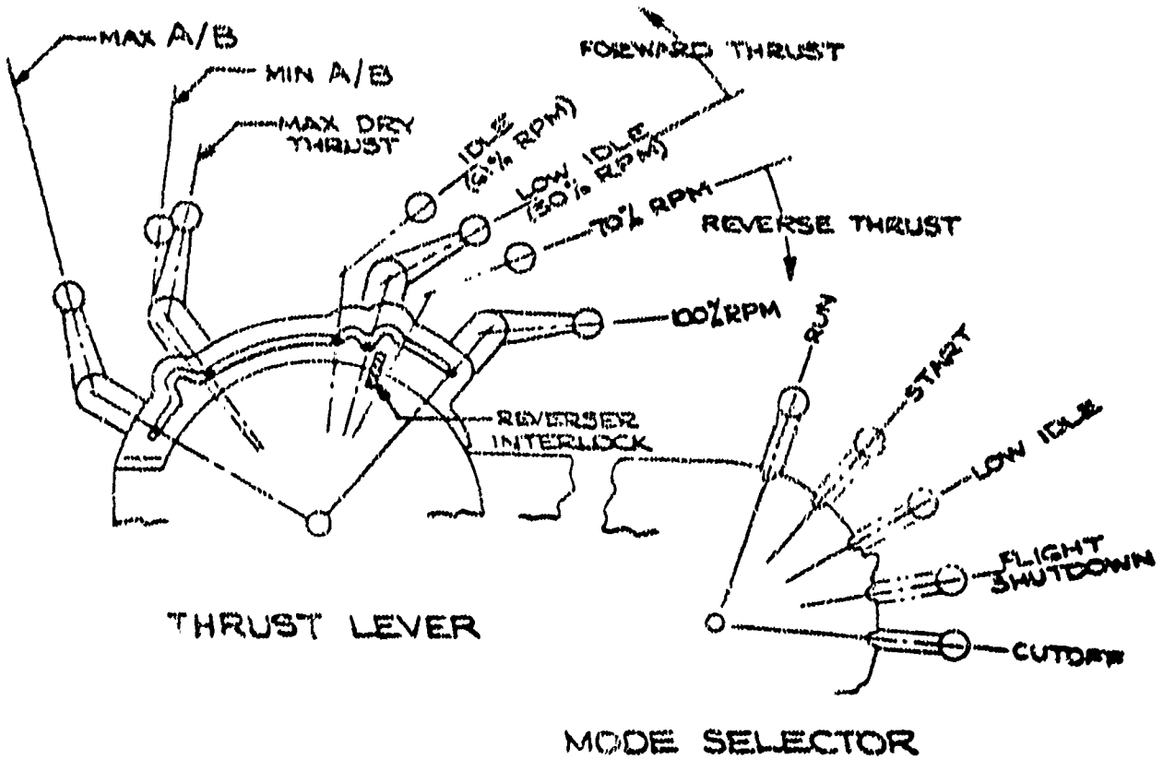

Fig 21 Thrust Control Lever Schematic

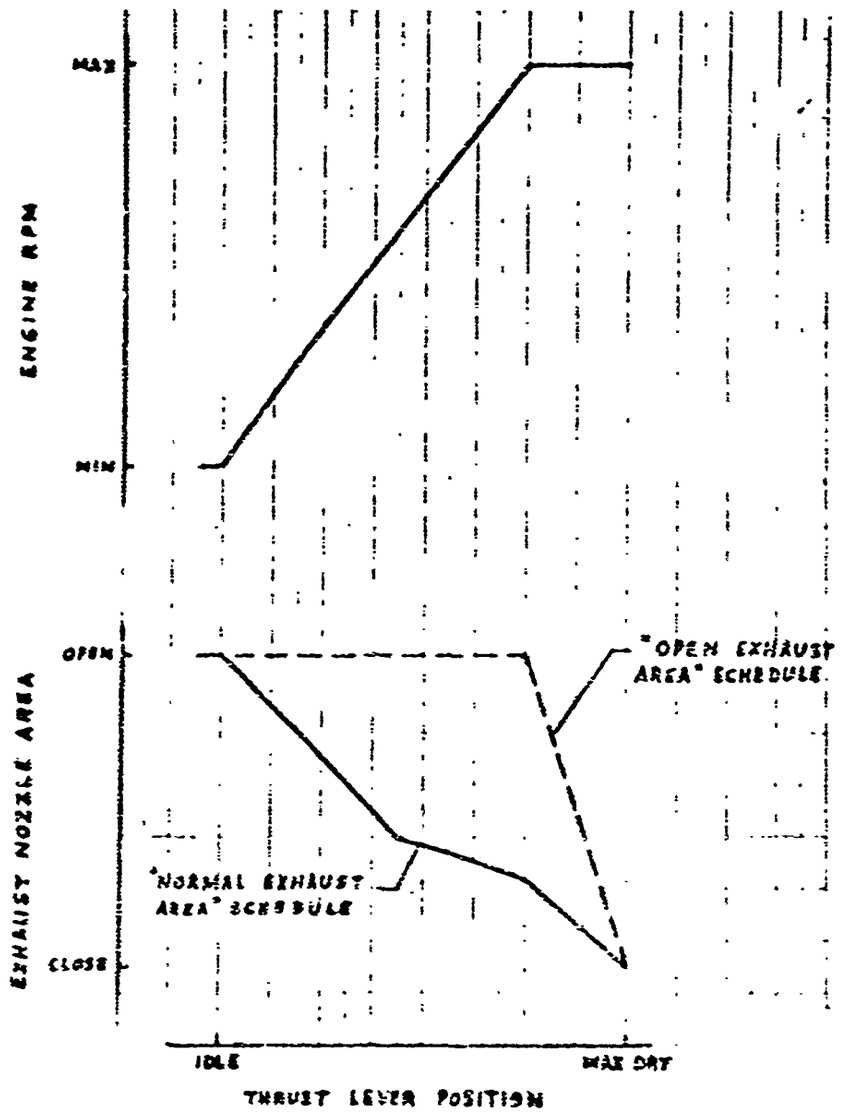

Fig 26 Exhaust Area and RPM Schedules

rpm schedule is also shown on Fig. 26. The 100-percent rpm flat permits sufficient travel of the thrust lever during open-exhaust-area operation. The engine performance with the normal area schedule has not been affected.

6.3 ENGINE TRIMMING DURING NONSTANDARD DAYS

The trimming of engine rpm on a cold day is designed to be performed manually, as described in the Phase II-A Propulsion Report. The capability of increasing total engine airflow during hot days has been added to the system by utilizing the excess capacity of the nozzle secondary air system. The secondary air system is controlled through modulation of the secondary air control valves on the engine. During hot-day cruise operation, the nozzle secondary air system, which bypasses air from the engine face back to the exhaust nozzle, is used to handle the excess inlet air, thereby reducing the inlet bypass drag. The nozzle secondary air system is sized by maximum afterburning power at transonic speeds and has the capability of bypassing 10 percent of engine air at cruise. Normal cruise secondary air required is 3 percent. On a standard +15°F day, total air through the secondary air system is 7 percent. The normal secondary air control schedule is shown in Fig. 27. A bias to the schedule for hot-day operation is also shown. This bias signal will be transmitted to the engine from the flight deck by manual control.

Manual control is used to trim the engine to match the inlet airflow during supersonic cruise. Sufficient trim is available to account for airflow variations due to hot- and cold-day operation as well as inlet and engine airflow tolerance effects. The control reduces engine rpm (on a cold day) and increases secondary airflow (on a hot day).

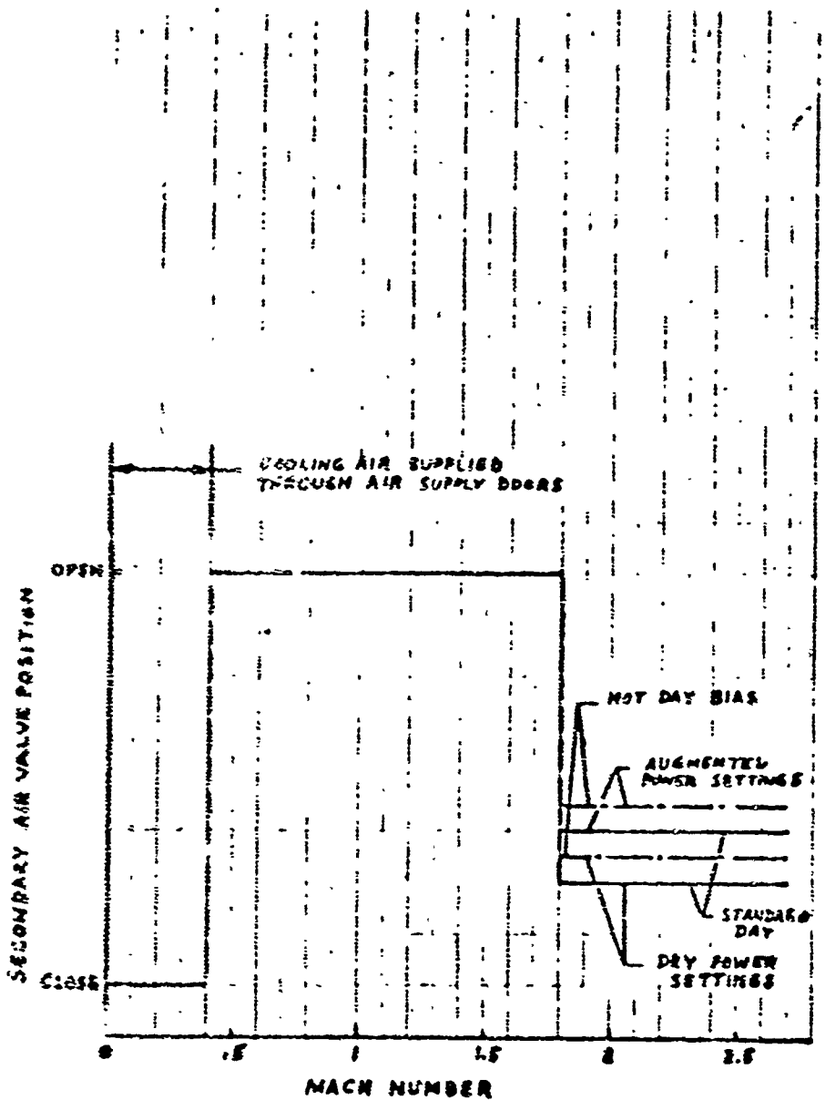

Fig. 27 Secondary Air System Cost of Schedule

7.0 EXHAUST SYSTEM

7.1 EXHAUST FLOW FIELD

The low-speed tests conducted during Phase II-A indicated that jet deflection would not cause a tail surface heating problem. Since Phase II-A, test data have been obtained to define the exhaust flow field at supersonic speeds. As a result of these tests, the 5-degree bend in the nozzle has been removed, and the horizontal tail on the 733-390 configuration has been positioned below the engine exhaust plume. For these tests, a nozzle model was constructed using a kerosene-oxygen-air burner to simulate the exhaust flow at Mach 2.7. Nozzle contour, total to free-stream pressure ratio, and velocity ratios were duplicated for the full-scale maximum dry power and maximum afterburning conditions. The model was an isolated nacelle with no inlet flow and with no wing or body present. The exhaust nozzle was canted 0, 6, and 12 degrees. Temperature profiles were measured 10 nozzle-exit diameters downstream (the approximate location of the 733-290 horizontal tail hinge line).

The model installed in the Boeing supersonic wind tunnel is shown in Fig. 28. Fig. 29 is a schematic showing the orientation of the model with the tunnel flow and the exhaust temperature profile with respect to the jet axis. Temperature profiles are shown in Figs. 30 through 35. Correlation between θ and temperature in degrees F is shown in Fig. 36. Analysis indicates that the bending of the wake is reduced at lower Mach numbers.

To obtain more definitive data, a complete airplane model with four small (1-1/2 inch diameter) kerosene burners is under construction. This model will be tested over the transonic and supersonic speed regimes and wake data will be obtained at several positions downstream of the exit. These data will include all of the downwash, wing, and body interference effects to be expected on the full-scale airplane.

7.2 THRUST REVERSER

The first series of reverser ingestion tests were conducted during the month of August 1965. In the low-speed tunnel, 17 cascade configurations were tested. The three configurations having the lowest ingestion speeds are shown in Fig. 37. Fig. 38 shows a typical curve of the inlet air temperature versus airspeed for configuration A of Fig. 37. For this configuration, ingestion occurred at about 80 knots.

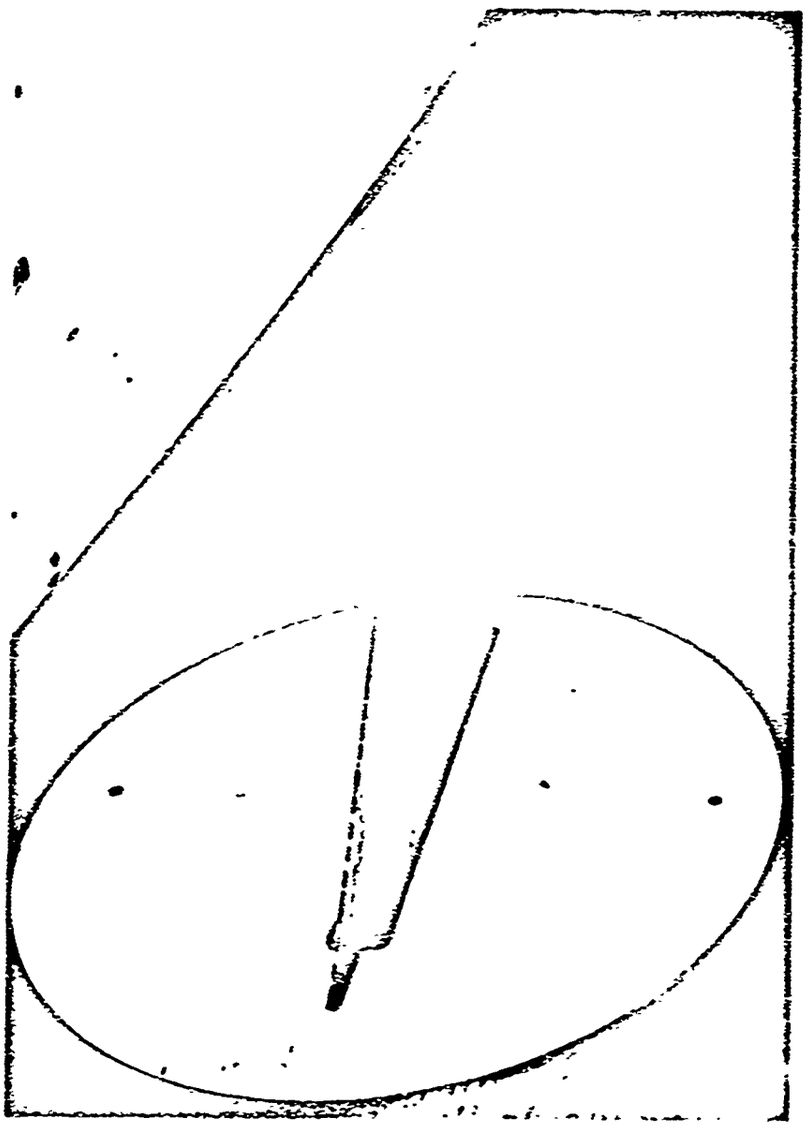

Fig. 28 Jet Wake Test Model

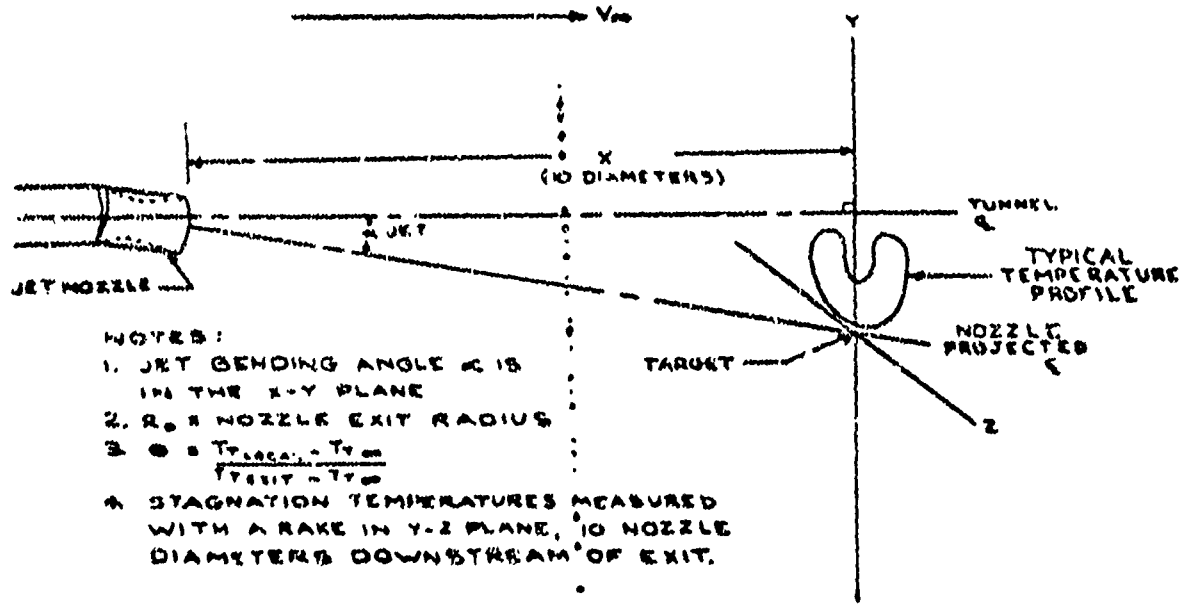

Fig. 29 Jet Wake Test Installation Schematic

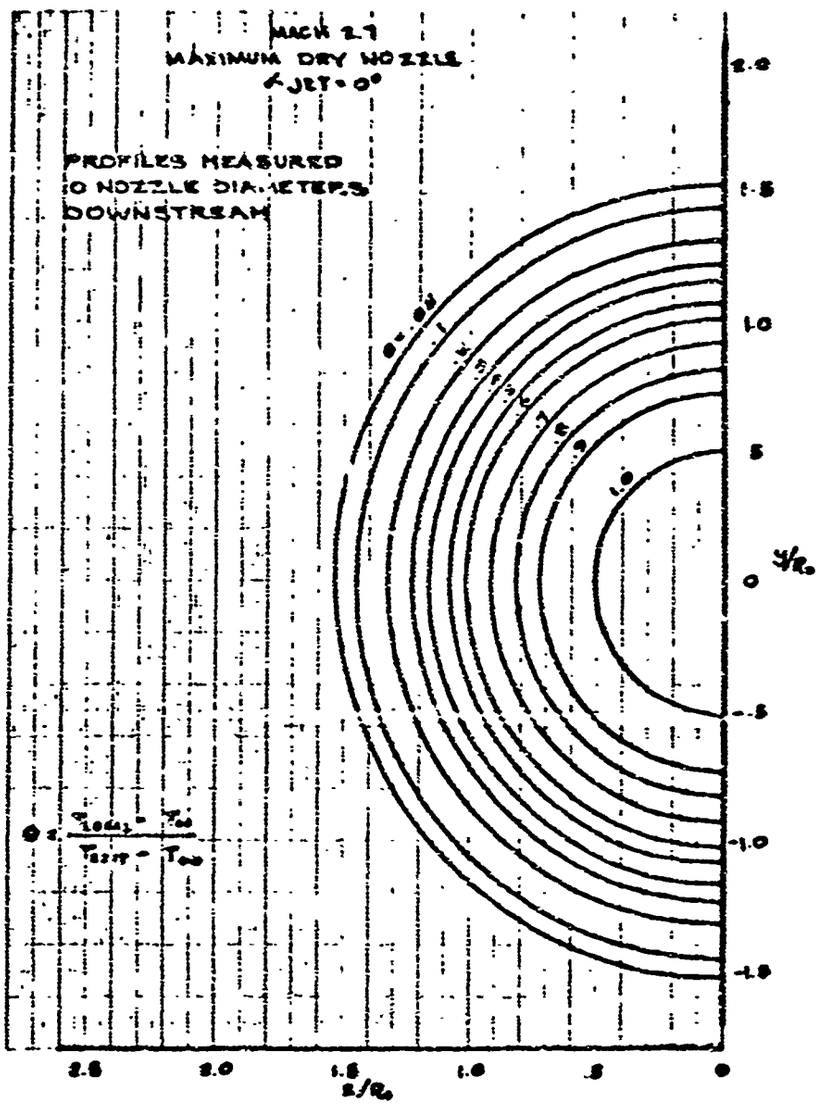

Fig. 30 Jet Wake Temperature Profile – Maximum Dry Nozzle, $\phi_{Jet} = 0°$

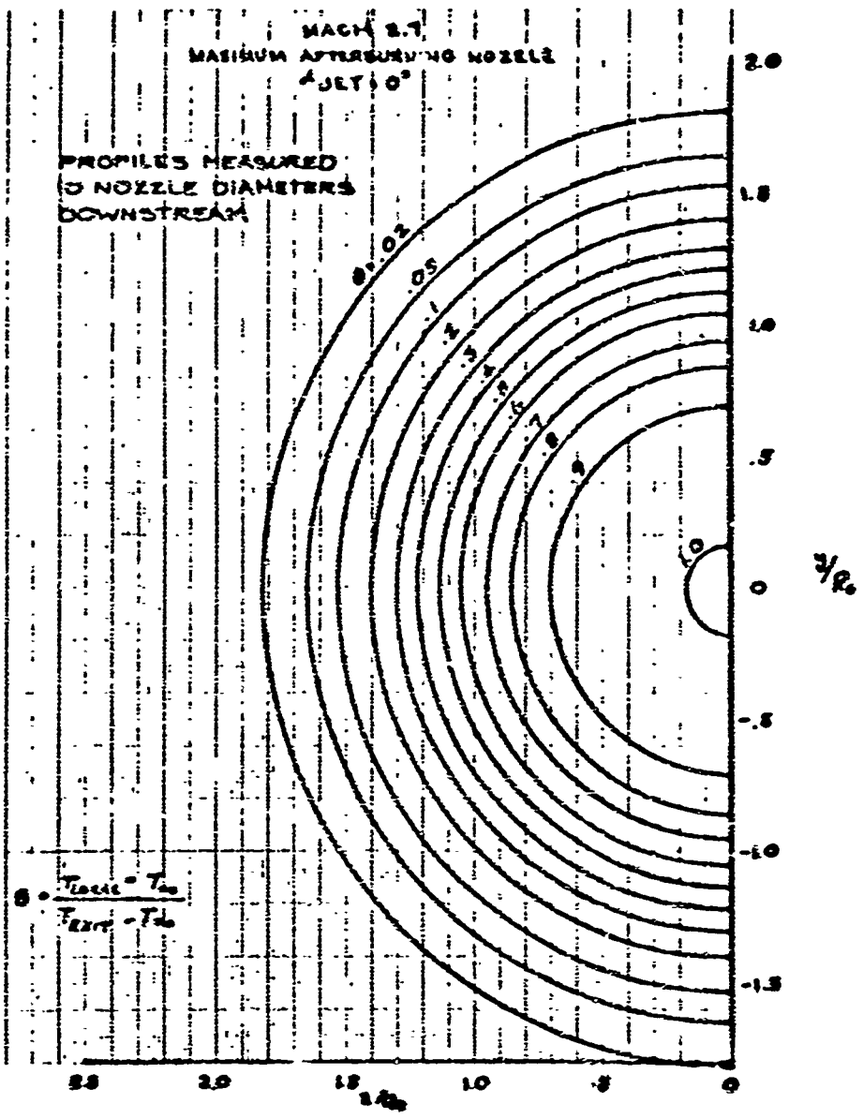

Fig. 31 Jet Plume Temperature Profile – Maximum Afterburning Nozzle, Jet = 0°

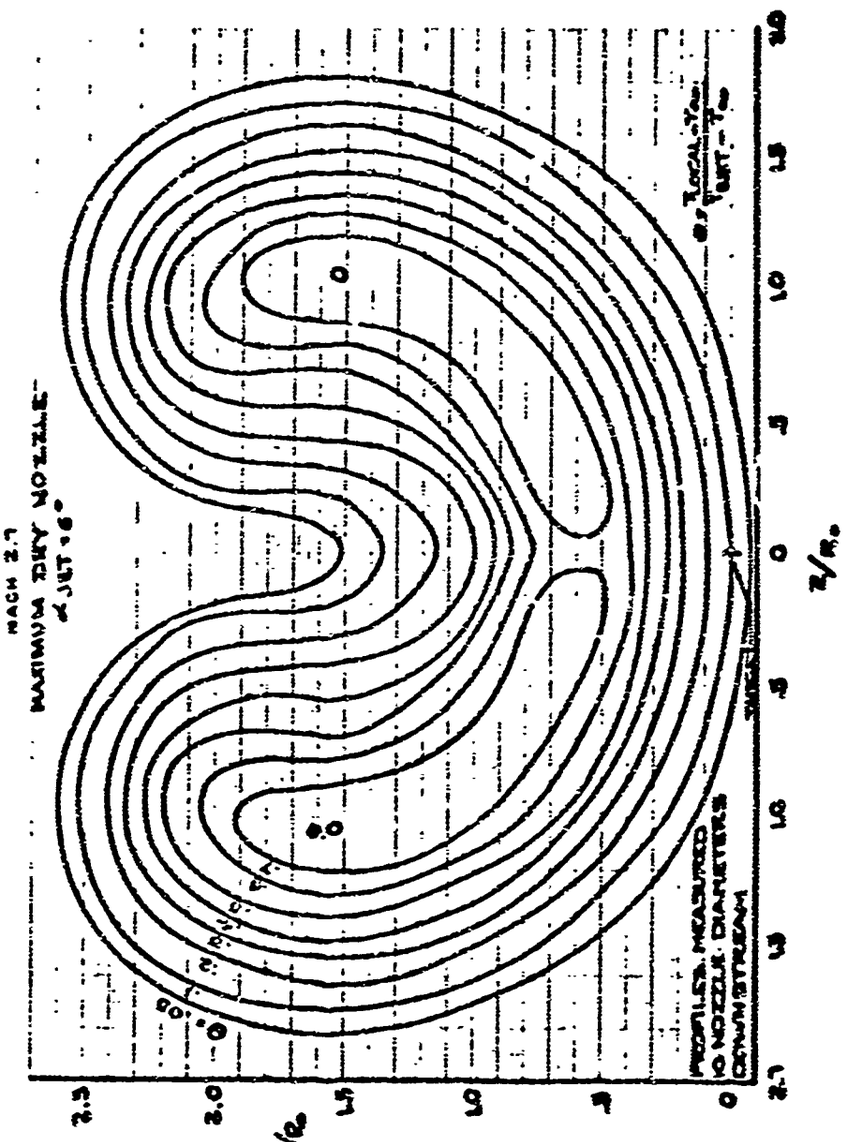

Fig. 32 Jet Wake Temperature Profile – Maximum Dry Nozzle, $\alpha_{Jet} = 6^{\circ}$

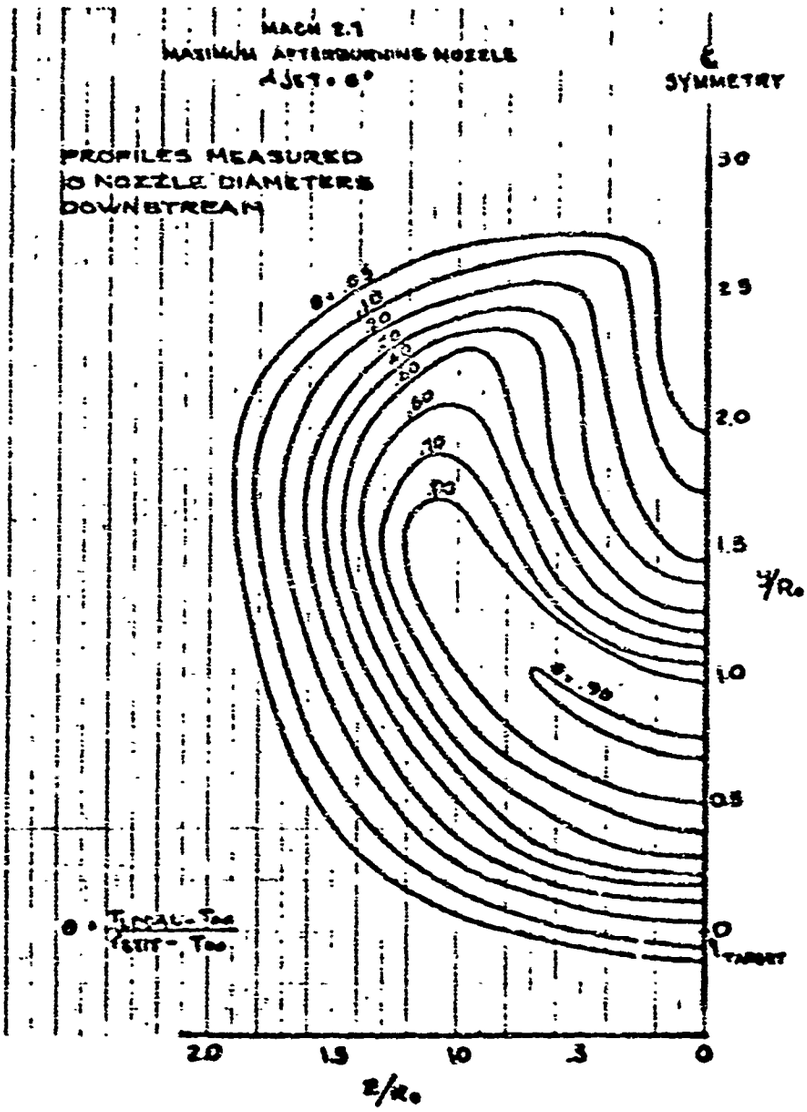

Fig. 33 Jet Wake Temperature Profile – Maximum Afterburning Nozzle, $\phi_{Jet} = 6°$

CR-11905

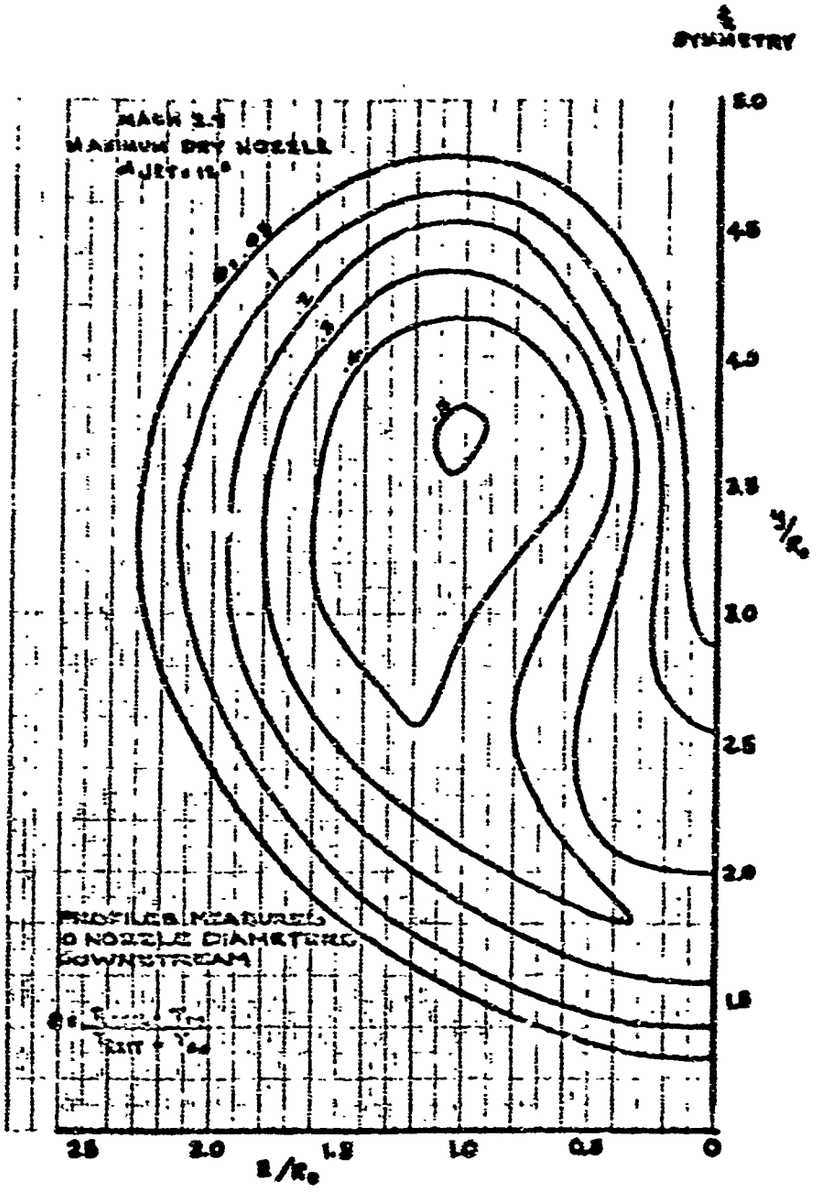

Fig. 34 Jet Wake Temperature Profile - Maximum Dry Nozzle, Jet = 12°

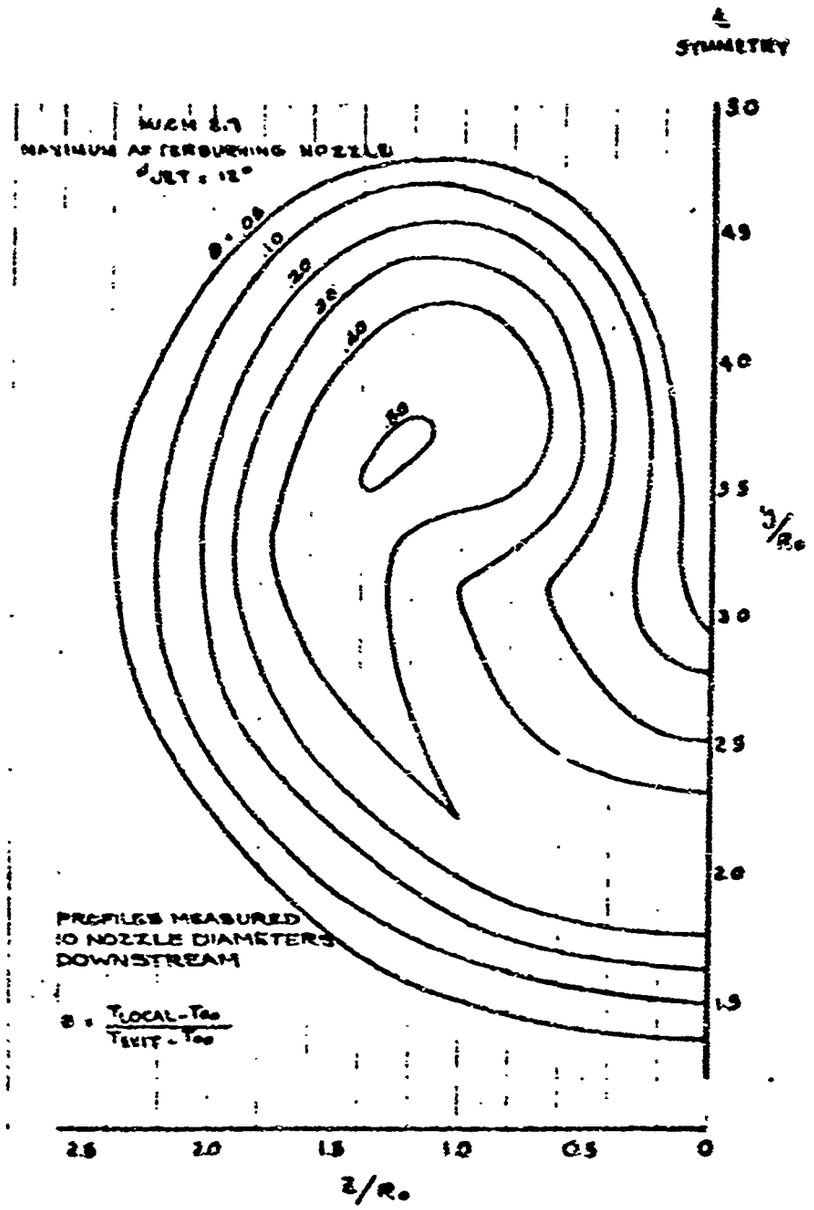

Fig. 35 Jet Rake Temperature Profile - Maximum Afterburning Nozzle, ϕ Jet = 12°

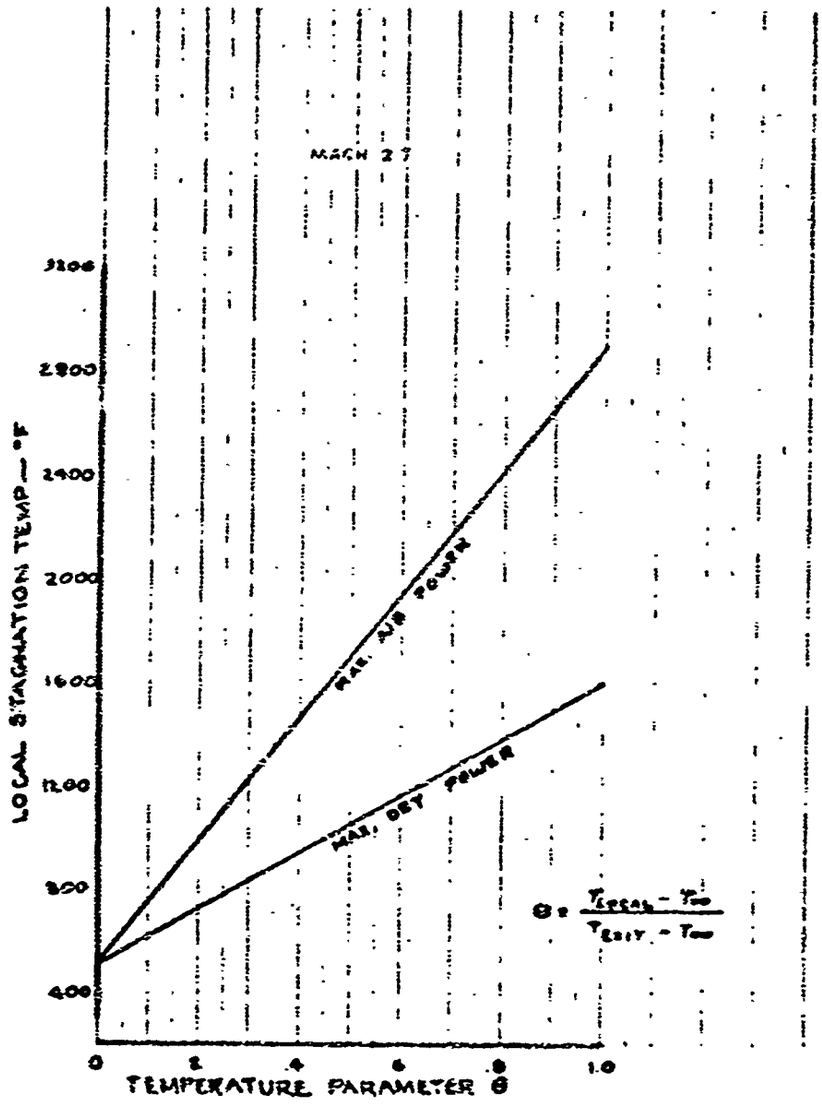

Fig. 18 Temperature Correction Factors For Jet Wake Temperature Profiles

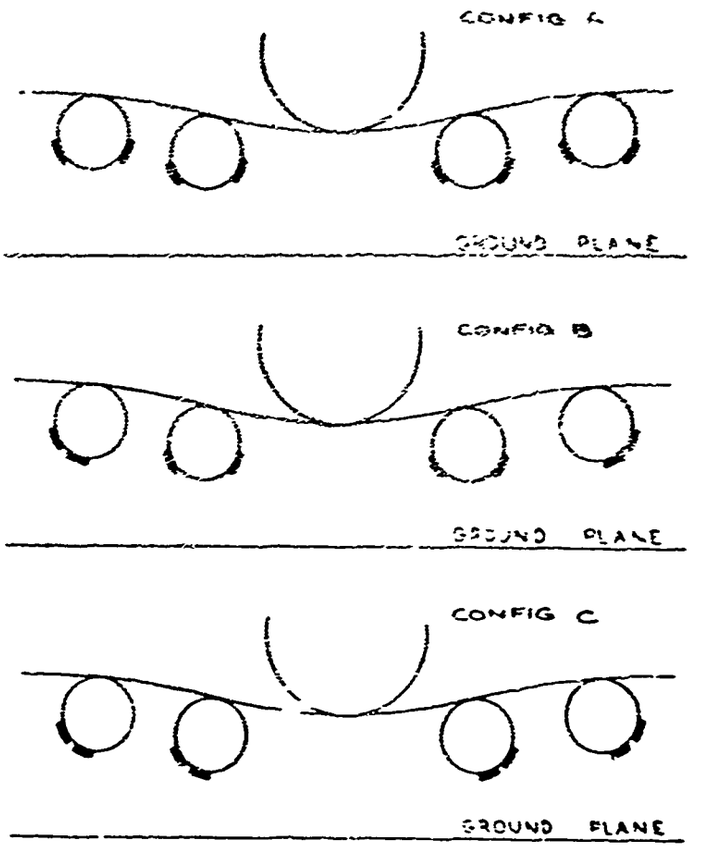

Fig. 37 Thrust Reverser Test Configurations

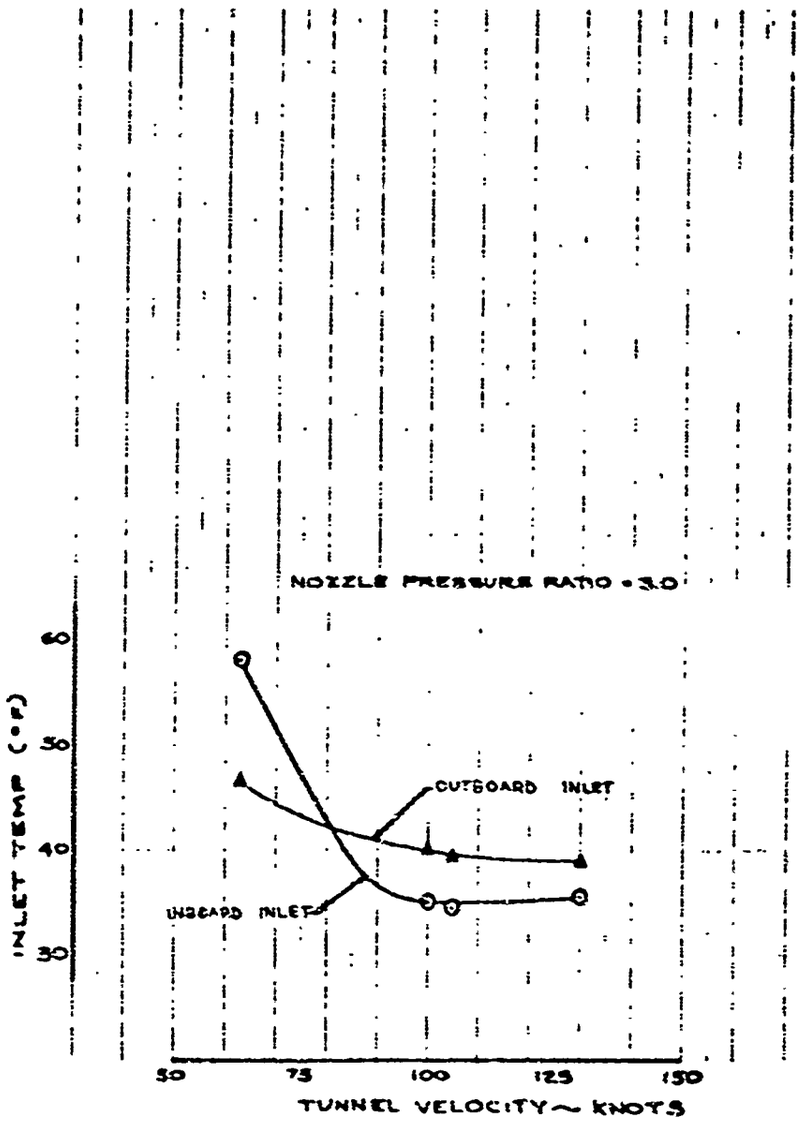

Fig. 35 Model Inlet Temperature Rise Due to Reingestion

8.0 NOISE

8.1 ENGINE NOISE CHARACTERISTICS

The noise characteristics of the GE4/J5G engine are presented in Fig. 39. These noise levels were obtained using the same procedures outlined in the Phase II-A report (D6-8680-7, Sonic Boom and Noise). However, some reductions have subsequently been made in the absolute noise levels. These changes are the result of incorporating the "open nozzle" concept (Par. 6.2) for power cutback during takeoff. In Phase II-A, this concept, used as a means of reducing landing noise, has been incorporated in the engine at this time to provide noise reduction during climbout as well as during landing. In principle, the open nozzle allows the engine to provide the same thrust at lower jet velocities than would be possible under the "standard nozzle" schedule. The lower jet velocity results in less jet noise being generated. At 50 percent of maximum dry thrust, and with the exhaust nozzle wide open, the jet noise is 3 PNdb less than that previously quoted. With the nozzle wide open, the suppression effect of the star-shaped primary and ejector is reduced, but the overall effect is a reduction in noise.

8.2 ENGINE NOISE SUPPRESSION TESTS

A series of model tests has been conducted to achieve maximum noise suppression from a nozzle-ejector configuration of the type designed by the General Electric Company for their SST engine. The effects of star-shaping the primary nozzle and varying the ejector throat and exit diameters were investigated. The nozzle configurations tested are shown in Fig. 40. The dimensions of the nozzles and ejectors tested are presented in Fig. 41. Noise suppression, relative to a standard convergent round nozzle, varied from 1 to 3 PNdb. A complete report of these tests is given in Ref. 5.

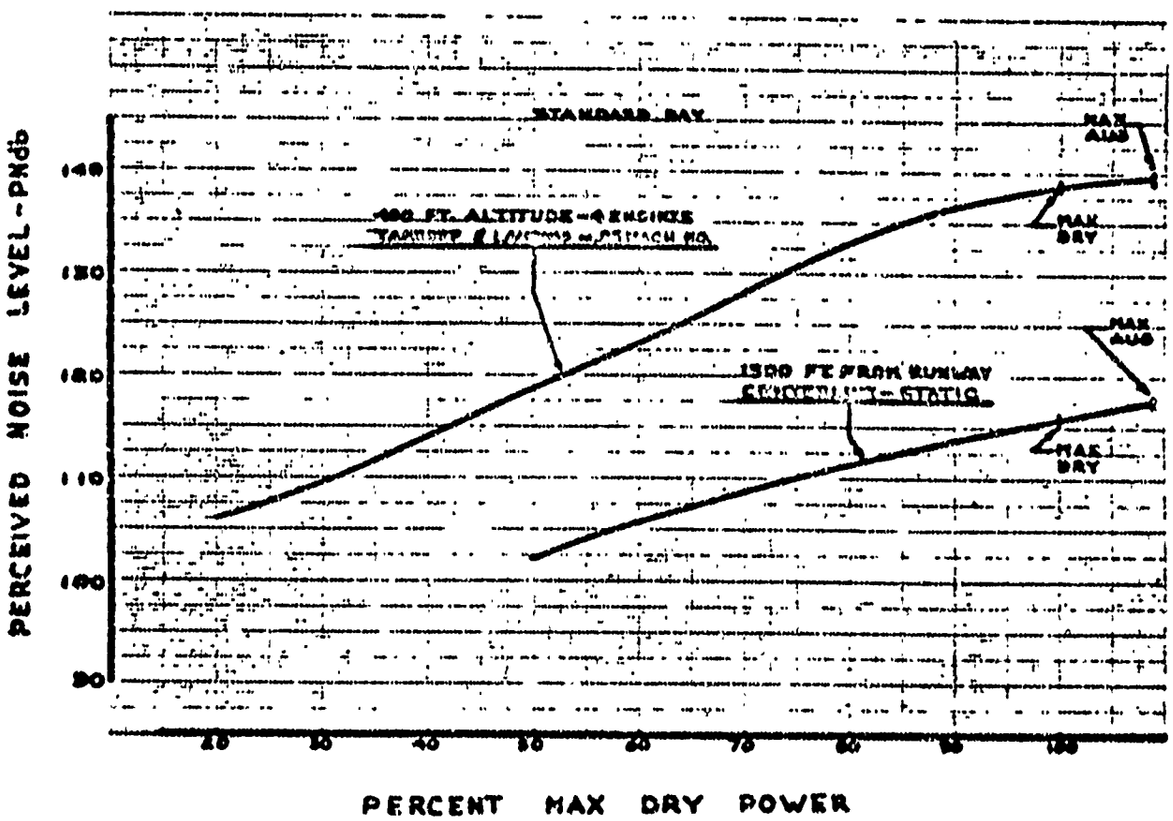

Fig. 39 Noise Characteristics for the GE4/J5G Engine

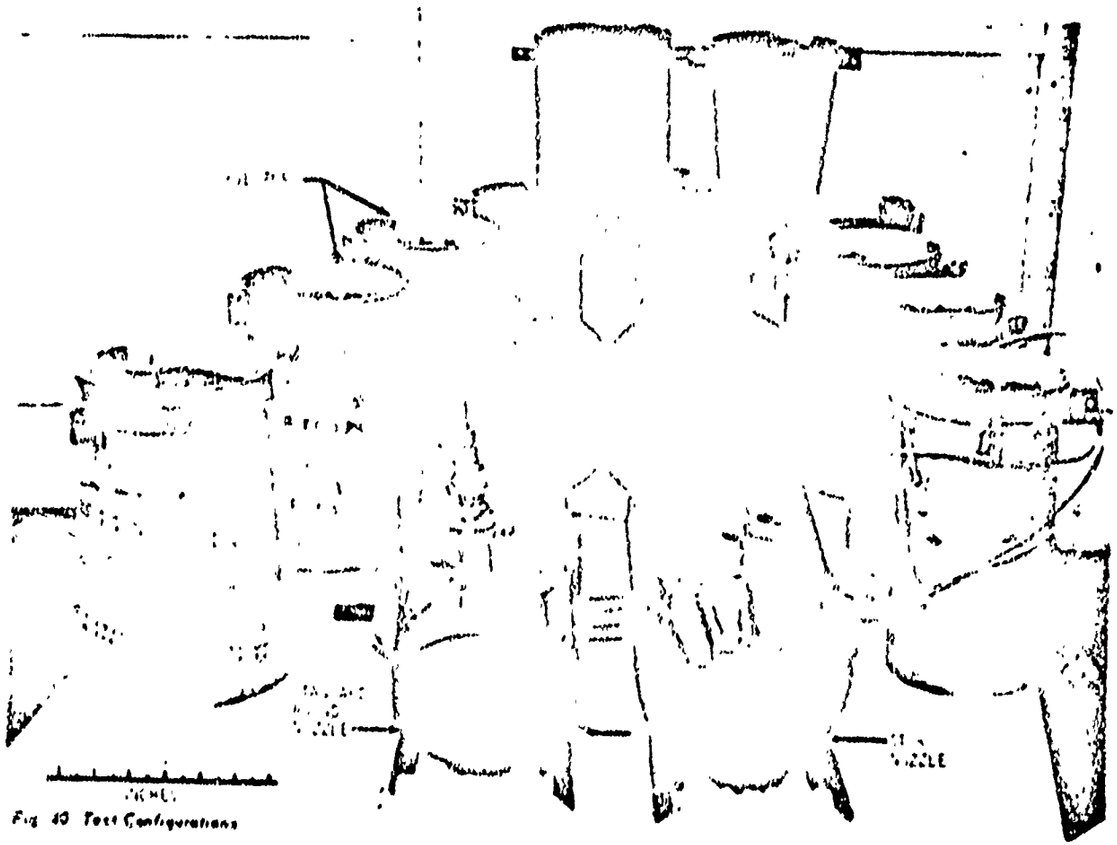

Fig 40 Test Configurations

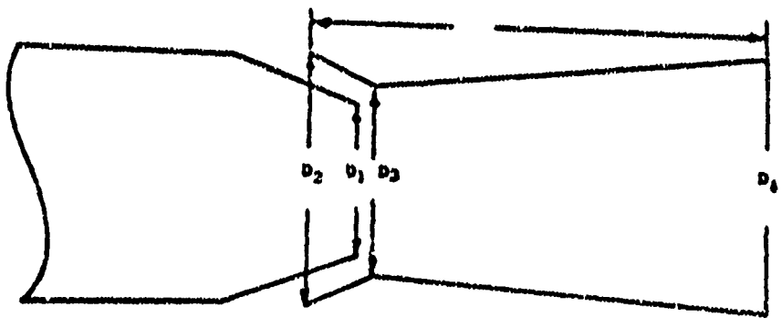

	NOZZLE		EJECTORS										
DIM. in.	STAR	STAND.	#1	#2	#3	#4	#5	#6	#7	#8	#9	#10	#11
D_1	*4.07	4.25											
D_2			5.00	5.25	5.25	5.25	5.00	5.5	5.5	5.75	5.75	5.75	5.50
D_3			4.5	4.75	4.75	4.75	5.0	5.0	5.0	5.25	5.25	5.25	5.00
D_4			5.0	5.0	5.25	5.5	5.25	5.5	5.5	5.50	5.5	5.5	5.50
L			10.0	10.0	10.0	10.0	10.0	10.0	10.0	10.0	10.0	10.0	10.0

* DIAMETER OF EQUIVALENT AREA ROUND NOZZLE
MAXIMUM STAR DIAMETER = 4.4 inches
MINIMUM STAR DIAMETER = 3.88 inches

Fig. 41 Nozzle and Ejector Dimensions

9.0 FUEL SYSTEM

Changes in the fuel system have been made in tank capacity and shape, tank locations, and more efficient use of tank insulation. These changes are described in the following paragraphs. There have been no changes that would affect either safety or the use of commercial kerosene fuel.

9.1 FUEL TANKS

Structural cavities within the lower lobe of the airplane body, inner wing, movable wing, and wing center section are still used to contain fuel, as shown in Fig. 42. The usable fuel capacity is 260,764 pounds (38,920 U.S. gallons) of commercial aviation kerosene. Tank capacities in U.S. gallons are:

Main No. 1	5,560
Main No. 2	9,295
Main No. 3	11,035
Main No. 4	5,560
Left-Hand Auxiliary	3,735
Right-Hand Auxiliary	3,735

The primary changes to the fuel tanks are:

- The fuel volume in the inner wing has been increased by moving Main No. 2 forward and reducing the size of the main landing gear wheel wells. This permits eight forward and three aft body fuel bladder cells to be eliminated. This was done to save weight in bladder cells and pressurized cabin flooring.

- The payload-range trade fuel has been redistributed such that each main tank now contains some of this fuel, with the largest portion in Main No. 3. This arrangement reduces the center-of-gravity movement for a full fuel mission (see fig. 43). In Phase II-A, all of the payload-range trade fuel was contained in Main No. 2.

9.2 TANK INSTALLATION

Main No. 1 and the auxiliary tanks are now insulated only on the lower skin between stiffeners, as shown on Fig. 44, but still maintain the same fuel temperature at the end of cruise as for Phase II-A. With the 733-390 fuel management, the upper surfaces of these tanks dry early in flight. This provides an insulating air gap that makes upper-surface insulation much less effective than lower-surface insulation. The heat flux to the fuel through the lower stiffeners is small compared to that between stiffeners. It was found that overall weight saving was obtained by replacing stiffener insulation with a slight increase in lower skin insulation. For these reasons this method is significantly less expensive, provides additional fuel volume and reduces weight.

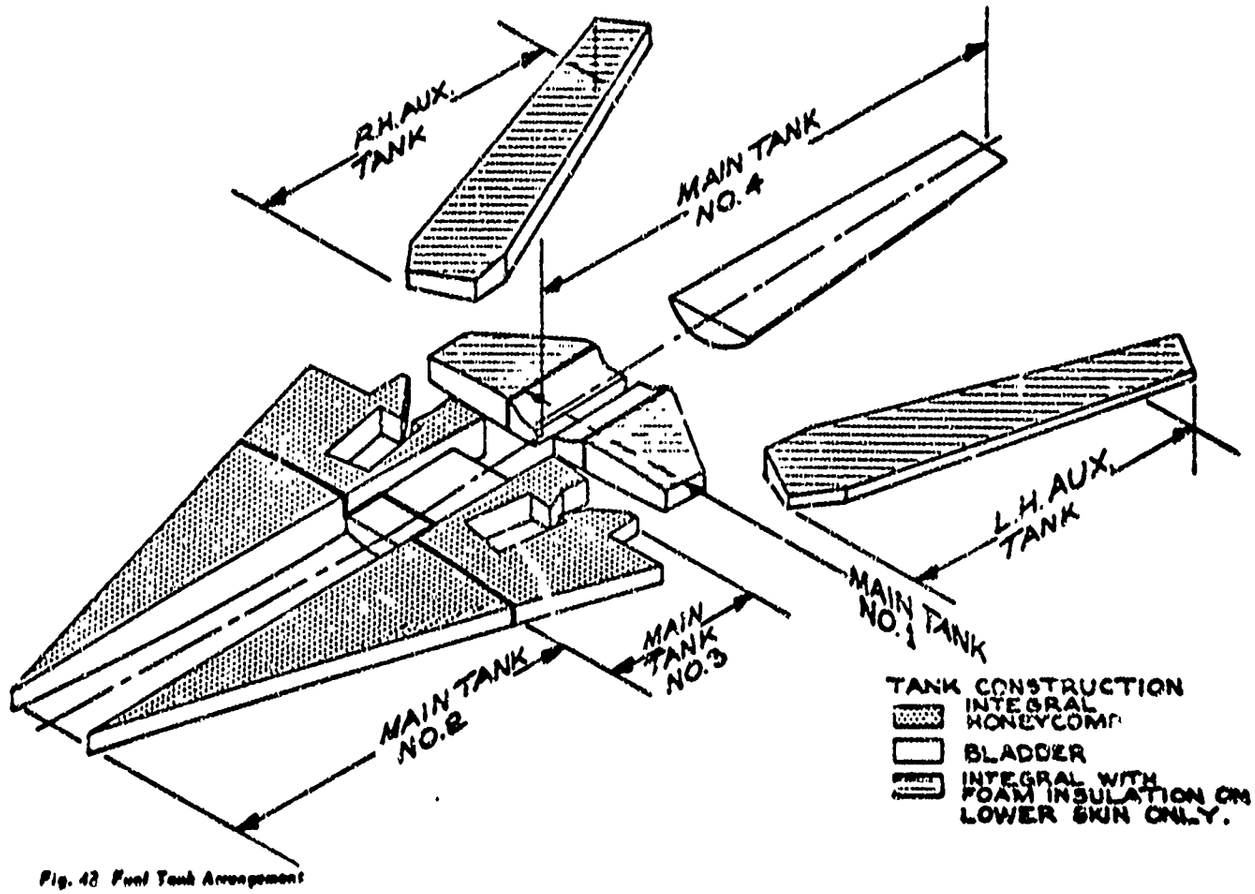

Fig. 42 Fuel Tank Arrangement

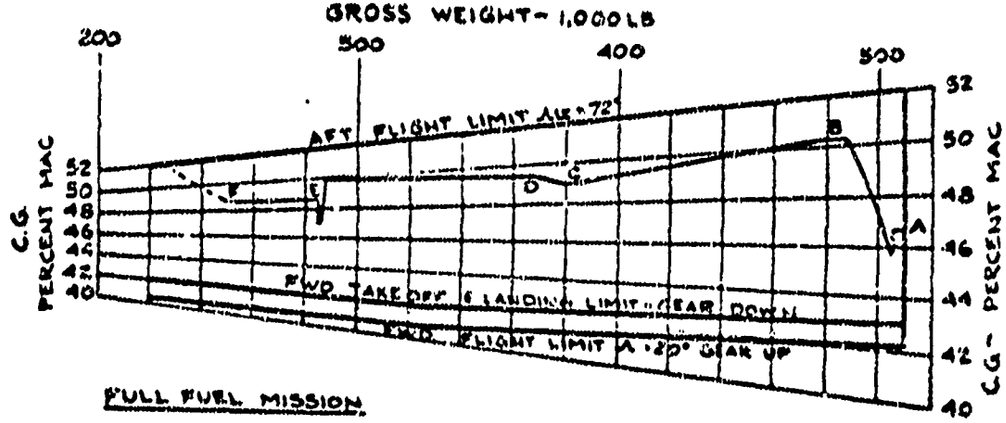

FULL FUEL MISSION.

--- PAYLOAD (19,756 POUNDS)

FUEL USE

A-B TAKEOFF AND CLIMB ON MAINS EQUALLY. RETRACT GEAR, SWEEP WING TO 72°

B-C USE OUTBOARD AUXILIARY FUEL EQUALLY WITH MAINS 2 & 3 UNTIL AUXILIARY TANKS ARE EMPTY.

C-D FEED ALL ENGINES FROM MAIN TANK 3 THROUGH CROSS FEED MANIFOLD UNTIL ALL MAINS ARE EQUAL.

D-E CONTINUE CRUISE, DESCEND AND LAND USING MAINS EQUALLY. (WING SWEEP OF 20°, GEAR DOWN AT E).

E-F RESERVE FUEL DISTRIBUTED EQUALLY IN MAIN TANKS.

Fig. 43 Commercial Gravity Travel – Full Fuel Mission

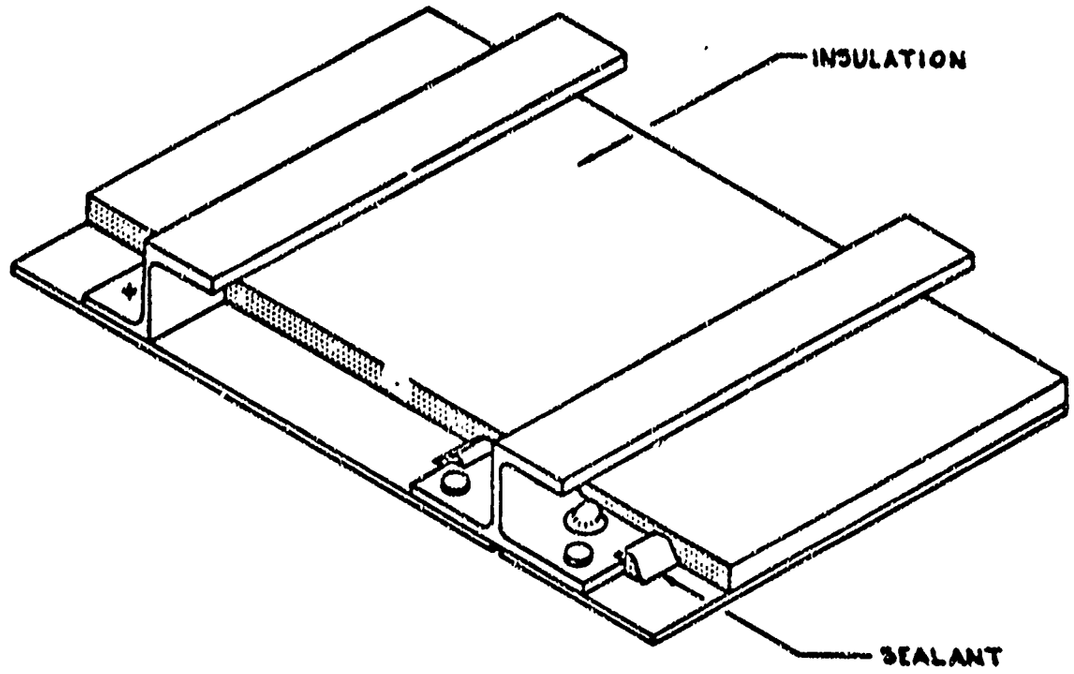

Fig. 44 Typical Integral Wing Tank Skin Panel Construction

9.3 ENVIRONMENT TEST

Simulated 4000-statute-mile flight cycle environment tests are being conducted on a test tank using FA-S-1 fuel (low-thermal-stability kerosene). The test tank is representative of the auxiliary tanks having upper and lower titanium skins, stiffeners, and rib chords. The lower skin is insulated between stiffeners only. After 50 cycles, the appearance of the insulation was unchanged and there were no visible deposits on either the insulated lower surface or the bare upper surface.

REFERENCES

1. General Electric GE4/J5G Model Specification E-2040B, November 1, 1965

2. General Electric Performance Data Deck R65FPD159, June 17, 1965

3. D6-19905, Air Induction Control System Performance Specification, November 1, 1965, The Boeing Company

4. D6-19908, Propulsion Controls Performance Specification, November 1, 1965, The Boeing Company

5. T6-3483, The Effect of Ejector Design Parameter Changes on the Acoustic Performance of Ejector-Nozzle Combinations, October 29, 1965, The Boeing Company

6. Pratt & Whitney Aircraft JTF17A-20B Preliminary Engine Specification 2681, October 30, 1964, Revised November 1, 1965

7. Pratt & Whitney Engine Performance Data Deck 5173 Low TIT, September 15, 1965

8. Pratt & Whitney Engine Performance Data Deck 5172 High TIT, September 15, 1965

9. D6-19906-1, Propulsion System Performance Specification, November 1, 1965, The Boeing Company

10. D6-19906-2, Propulsion System Performance Specification, November 1, 1965, The Boeing Company

9.3 ENVIRONMENT TEST

Simulated 4000-statute-mile flight cycle environment tests are being conducted on a test tank using FA-C-1 fuel (low-thermal-stability kerosene). The test tank is representative of the auxiliary tanks having upper and lower titanium skins, stiffeners, and rib chords. The lower skin is insulated between stiffeners only. After 50 cycles, the appearance of the insulation was unchanged and there were no visible deposits on either the insulated lower surface or the bare upper surface.

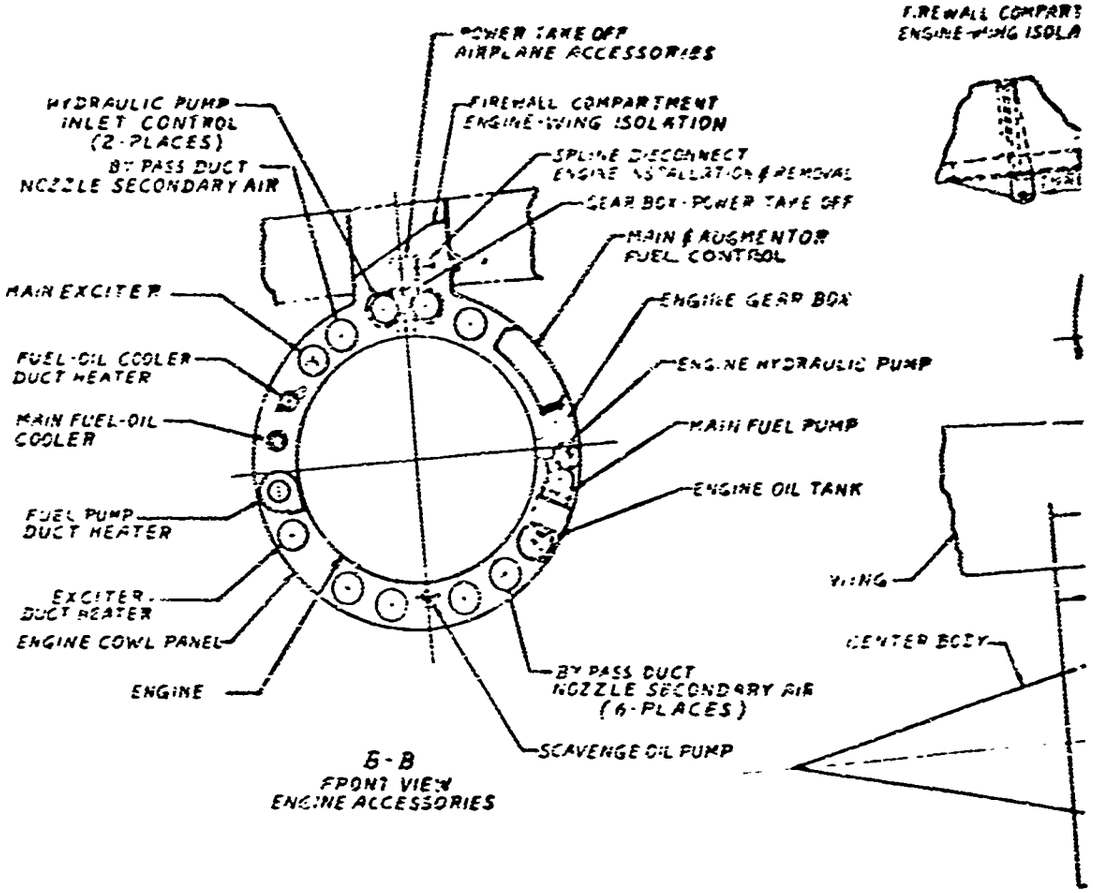

B-B
FRONT VIEW
ENGINE ACCESSORIES

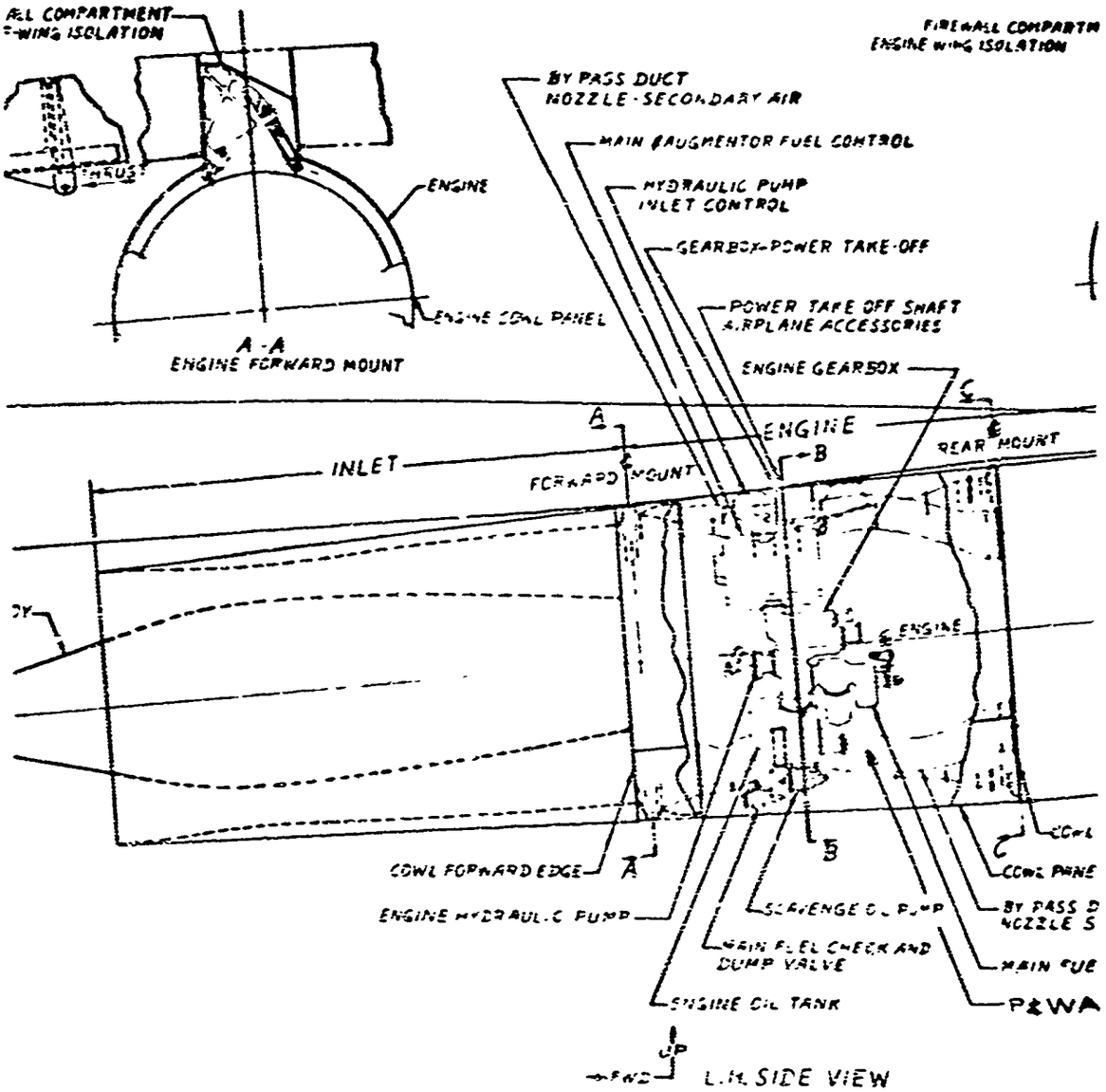

Fig 45 P&WA JTF17A

2

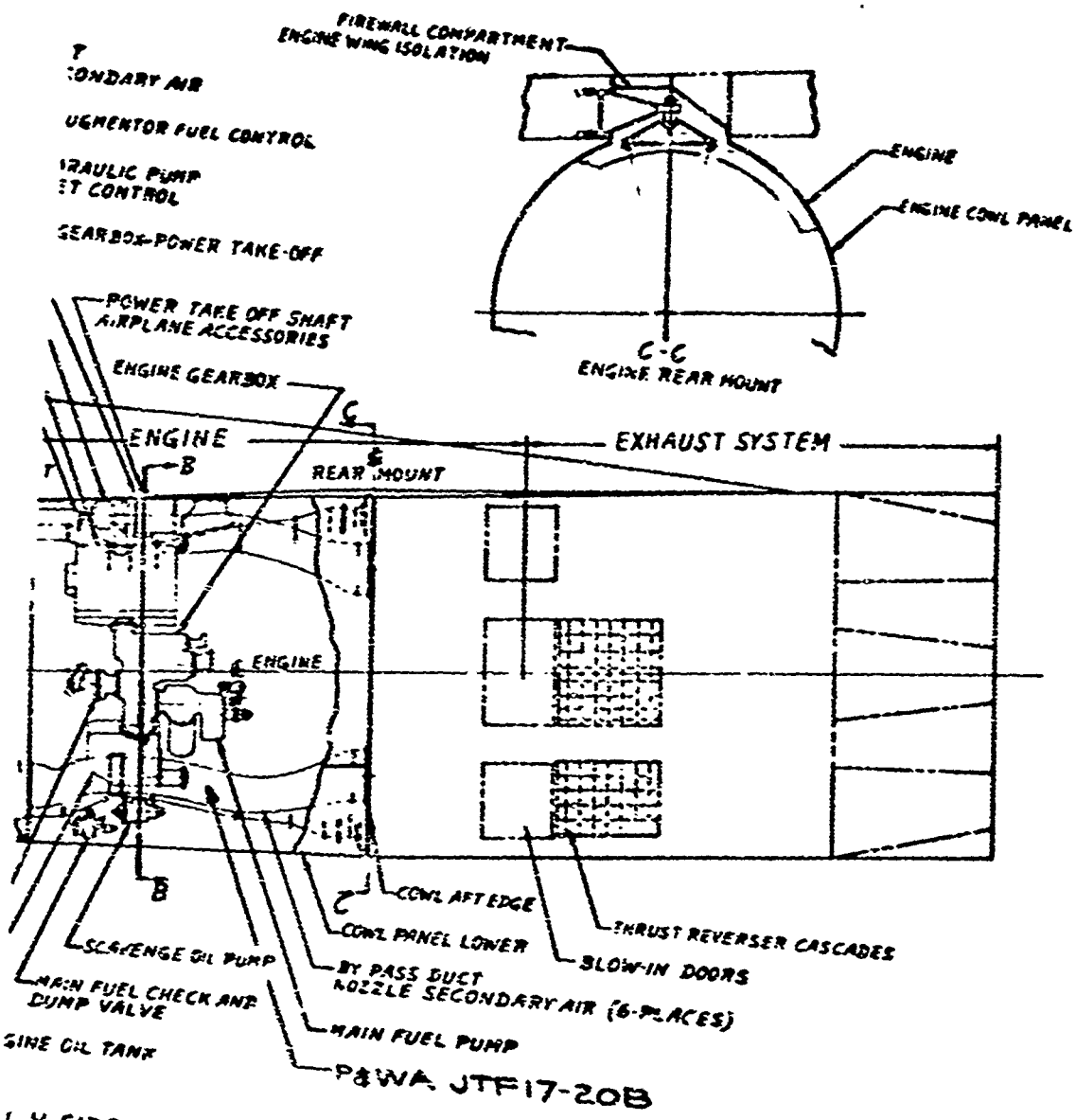

Fig. 45 P&WA JTF17A-20B Propulsion Pod

2.0 INSTALLED PERFORMANCE AND WEIGHT

The installed performance of the Pratt & Whitney JTF17A-20B engine is found in Document D6-19906-2, Propulsion System Performance Specification, November 1, 1965.

2.1 ENGINE WEIGHT

The weight of the JTF17A-20B engine at 650 pounds-second airflow size for either the 1900°F or 2200°F version is 10,100 pounds as specified in the engine model specification (Ref 5).

The following Boeing installation features are included in the installed engine weights:

	Pounds
Mounting Strut	147
Engine Mounts	108
Wing Attachment Fittings	205
Firewall and Seals	30
Brackets and Supports	22
Miscellaneous	48
Engine Weight	10,100
TOTAL INSTALLED ENGINE WEIGHT	10,660 Pounds

Total installed propulsion pod weight is as follows:

Wing Modifications for Reverser	240
Inlet	2,180
Cowling	190
Installed Engine	10,660
TOTAL PROPULSION POD WEIGHT	13,270 Pounds

2.2 ENGINE CHARACTERISTICS

Table C shows the design characteristics of the JTF17A-20B engine.

2.3 ENGINE PERFORMANCE

The JTF17A-20B engine performance is essentially the same as that supplied by Pratt & Whitney during Phase II-A except for an airflow size increase from 640 to 650 pounds per second. Ref. 6 contains the guaranteed performance for both the 1900°F and 2200°F versions. For all other operating conditions, the computer decks (Ref. 7 and Ref. 8) provide the estimated performance with installation corrections.

The performance data are based on the 1962 U.S. Standard Atmosphere and geometric altitude.

Table C Engine Characteristics

	1900°F/2000°F Rating	2200°F/2300°F Rating
Sea Level Static Standard Day Thrust (No Losses) (pounds)		
Maximum Augmented	52,300	56,800
Maximum Dry	32,100	36,700
Engine Dry Weight, including Exhaust Nozzle and Thrust Reverser (pounds)	10,100	10,100
Thrust/Weight (Sea Level Static)		
Maximum Augmented	5.2	5.6
Maximum Dry	3.2	3.6
Net Thrust/Weight (Transonic Mach = 1.2, 45,000 feet)		
Maximum Augmented	1.7	1.8
Design Mach Number	2.7	2.7
Supersonic Cruise SFC		
Mach 2.7, 65,000 feet	1.58	1.50
Fan Recovery = 0.90		
Subsonic Cruise SFC		
Mach 0.8, 40,000 feet	0.98	1.03
Fan Recovery = 0.986		
Loiter SFC		
Mach 0.43, 15,000 feet	1.06	1.07
Fan Recovery = 0.986		
Acceleration Net Thrust (pounds)		
Mach 1.2, 36,150 feet	26,200	28,200
45,000 feet	17,000	18,300
55,000 feet	10,300	11,100
Reverse Thrust (Percent Maximum Dry Power)	50	50
Turbine Inlet Temperature (Nominal) (°F)		
Takeoff	2,000	2,300
Supersonic Cruise	1,900	2,200
Transonic Acceleration	2,000	2,300

Table C Engine Characteristics (Cont)

	1900°F/2000°F Rating	2200°F/2300°F Rating
Augmentation Temperature (Nominal) (°F)		
Takeoff	3,100	3,100
Supersonic Cruise	3,100	3,100
Transonic Acceleration	3,100	3,100
Bypass Ratio	1.3	1.3
Compressor Pressure Ratio	12:1	12:1
Fan Pressure Ratio	2.7:1	2.7:1
Initial Time Between Overhaul	600 hours	600 hours

3.0 NOISE

The noise characteristics of the Pratt & Whitney JTF17A-20B engine with 2000°F takeoff turbine inlet temperature are presented in Fig. 46. These noise levels were obtained by the same procedures outlined in the Phase II-A report, D6-8680-7 Sonic Boom and Noise, except that a jet noise suppression of 4 db per octave band has been assumed. This noise suppression has been estimated by Pratt & Whitney for the blow-in-door ejector on the basis of noise measurements obtained from engine ground tests and airplane flyovers. Fig. 47 presents noise characteristics for the 2300°F turbine inlet temperature engine.

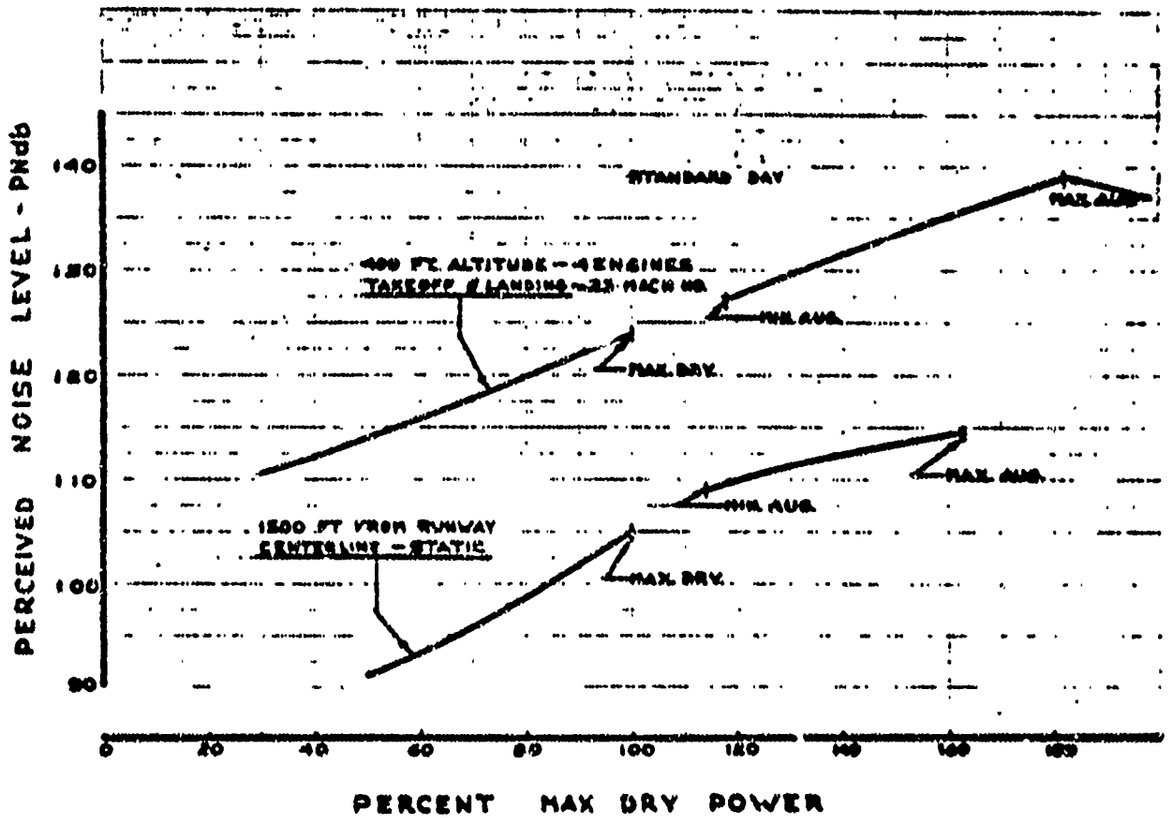

Fig. 46 Noise Characteristics For The P&WA JTF17A-208 Engine—2000°F Maximum Rating

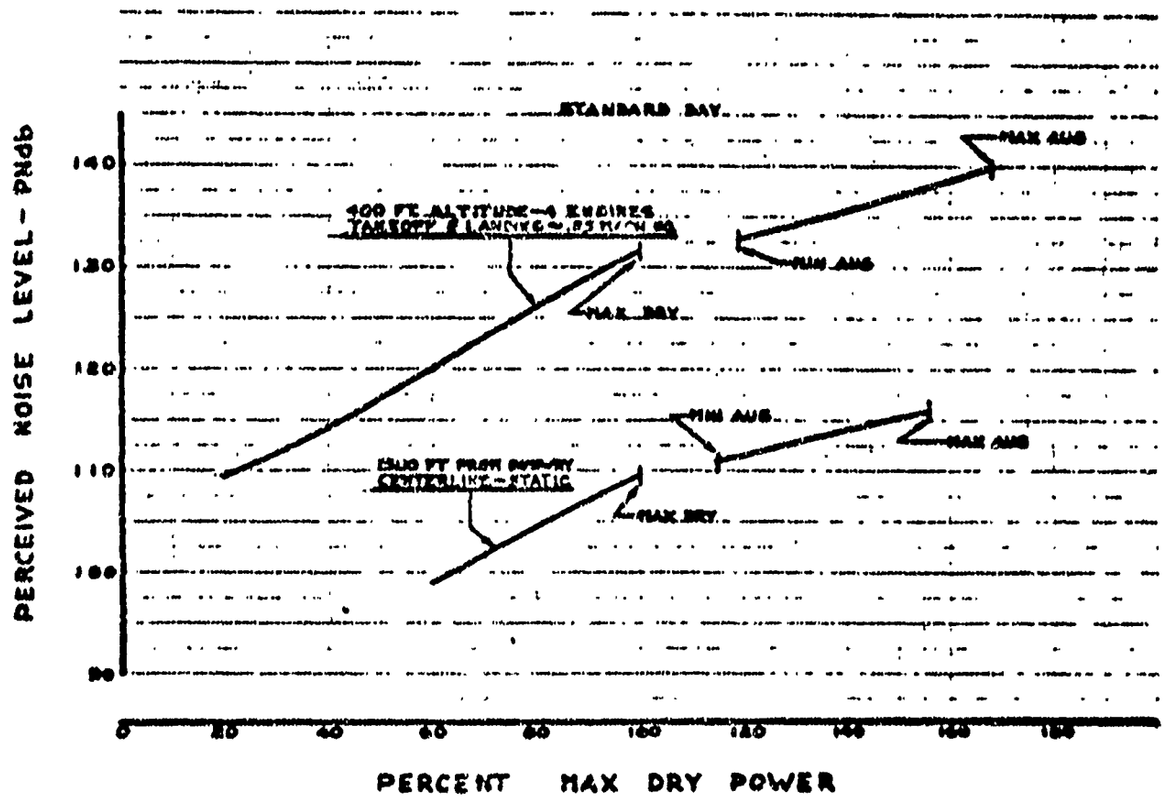

Fig. 47 Noise Characteristics For The PCWA JT8D7A-20B Engine—2300°F Maximum Rating